UNIVERSITÀ
DI PAVIA

Dipartimento di Biologia e Biotecnologie
"Lazzaro Spallanzani"

Laurea Magistralis in Molecular Biology and Genetics

Study of the mechanism of action of the anti-*Pseudomonas* compound PDSTP and analysis of its cytotoxicity

Supervisor:
Prof. Silvia Buroni

Co-supervisor:
Dr. Gabriele Trespidi

Experimental thesis by
Laura De Gregorio

Academic Year 2024/2025

TABLE OF CONTENTS

ABSTRACT

In cystic fibrosis, chronic *Pseudomonas aeruginosa* lung infections slowly destroy patients' respiratory function through colonization, biofilm formation, and antibiotic resistance which makes their treatment particularly difficult. The bacterium has multiple virulence factors including adhesins, secretion systems, siderophores, quorum sensing, and modified LPS to evade both host immune defences and antibiotic effect. Multidrug resistance, especially through efflux pumps and enzymatic inactivation, severely limits treatment options. There is a need for new antivirulence compounds blocking adhesion or boosting antibiotic efficacy to fill this gap.

PDSTP, a synthetic dispirotripiperazine derivative, was already known for blocking viruses like HSV and SARS-CoV-2, by completely saturating heparan sulfate proteoglycans (HSPGs) on cell surfaces. Recently, it showed strong anti-adhesion activity and antibiotic adjuvant effects against *P. aeruginosa*. With its four quaternary nitrogen atoms, PDSTP binds tightly to negatively charged molecules. However, PDSTP's mechanism of action was not clear, especially whether it targets bacterial LPS or host HSPGs, or both. Given its high polarity and inability to cross biological membranes, surface interactions represent the most plausible mechanism.

This Master thesis evaluated PDSTP safety and mechanism of action against *P. aeruginosa* PAO1. At first, cytotoxicity on human A549 lung cells was tested using MTT assay across concentrations 64-1024 µg/mL. Then, antibiotic adjuvant potential was assessed through checkerboard assays combining PDSTP (1-64 µg/mL) with ceftazidime or rifampicin, performed in presence/absence of LPS competitors (20 mM $MgCl_2$, 200 µg/mL purified LPS). Adhesion assays on A549 monolayers showed PDSTP anti-adhesion efficacy (25-200 µg/mL). Host HSPG dependency was tested using *B3GAT3*-knockdown A549 cells (genetic HS depletion) and Heparinase III-treated monolayers (enzymatic HS removal), both confirmed by immunofluorescence and flow cytometry.

PDSTP's cytotoxic profile showed over 95% A549 viability at 64-128 µg/mL and 80-85% at 256 µg/mL, establishing a wide therapeutic window that justified concentrations over 64 µg/mL for subsequent functional assays. Checkerboard showed

synergistic/additive interactions (FIC indices <0.5) with both ceftazidime and rifampicin under standard conditions, lowering inhibitory concentrations towards clinically achievable levels. Critically, both Mg^{2+} and exogenous LPS completely blocked PDSTP's adjuvant activity, restoring bacterial metabolic activity across all combinations.

PDSTP strongly blocked PAO1 adhesion (70-85% reduction at 50-200 µg/mL), confirming previous findings. This effect disappeared completely with LPS competitors ($MgCl_2$, purified LPS). However, on cells with no heparan sulfate (genetic or enzyme-treated), PDSTP still worked perfectly, and PAO1 adhesion remained unaffected. Flow cytometry confirmed >90% HS reduction in *B3GAT3*-knockdown cells (A549-610) cells and Heparinase III-treated monolayers.

All these experiments point to the same conclusion: PDSTP binds *P. aeruginosa* LPS through its phosphate groups. This destabilizes outer membrane integrity to facilitate antibiotic penetration, and stops bacterial-host interactions. Importantly, host HSPGs proved not to be involved for either PAO1 adhesion or PDSTP activity.

This study provides the evidence proposing PDSTP as a novel LPS-targeting compound working both as antibiotic adjuvant and anti-adhesion agent against *P. aeruginosa* in CF. By avoiding directly killing the bacteria, PDSTP minimizes resistance selection pressure while focusing on key pathogenesis steps. These findings warrant *in vivo* validation in CF models and structural studies of PDSTP-LPS interactions to guide similar development for clinical translation.

RIASSUNTO

Nella fibrosi cistica, le infezioni polmonari croniche da *Pseudomonas aeruginosa* distruggono lentamente la funzione respiratoria dei pazienti attraverso colonizzazione, formazione di biofilm e resistenza agli antibiotici, rendendo il loro trattamento particolarmente difficile. Il batterio possiede molteplici fattori di virulenza, tra cui adesine, sistemi di secrezione, siderofori, quorum sensing e LPS modificati, che gli consentono di evadere sia le difese immunitarie dell'ospite sia l'effetto degli antibiotici. La multiresistenza, in particolare attraverso pompe di efflusso e inattivazione enzimatica, limita severamente le opzioni terapeutiche. Esiste la necessità di nuovi composti anti virulenza che blocchino l'adesione o potenzino l'efficacia degli antibiotici per colmare questa lacuna.

Il PDSTP, un derivato sintetico della dispirotripiperazina, era già noto per bloccare virus come HSV e SARS-CoV-2 saturando completamente gli eparan solfato (HSPG) sulle superfici cellulari. Recentemente, ha mostrato una forte attività anti-adesione ed effetti adiuvanti antibiotici contro *P. aeruginosa*. Con i suoi quattro atomi di azoto quaternari, il PDSTP si lega fortemente a molecole cariche negativamente. Tuttavia, il meccanismo d'azione del PDSTP non era chiaro, in particolare se si leghi agli LPS batterici, alle HSPG dell'ospite o a entrambi. Data la sua alta polarità e l'incapacità di attraversare membrane biologiche, le interazioni di superficie rappresentano il meccanismo più plausibile.

Questa tesi magistrale ha valutato la sicurezza del PDSTP e il suo meccanismo d'azione contro *P. aeruginosa* PAO1. Inizialmente, è stata testata la citotossicità su cellule polmonari umane A549 mediante saggio MTT a concentrazioni di 64-1024 µg/mL. Successivamente, il potenziale adiuvante antibiotico è stato valutato attraverso saggi checkerboard combinando PDSTP (1-64 µg/mL) con ceftazidima o rifampicina, in presenza/assenza di competitori di LPS (20 mM $MgCl_2$, 200 µg/mL LPS purificato). I saggi di adesione su monocamere di A549 hanno dimostrato l'efficacia anti-adesione di PDSTP (25-200 µg/mL). La dipendenza dalle HSPG dell'ospite è stata testata utilizzando cellule A549 con knockdown di *B3GAT3* (deplezione genetica di HS) e monocamere trattate con Eparinase III (rimozione enzimatica di HS), entrambe confermate tramite immunofluorescenza e citometria a flusso.

Il profilo citotossico del PDSTP ha mostrato una vitalità delle A549 superiore al 95% a 64-128 µg/mL e dell'80-85% a 256 µg/mL, stabilendo una ampia finestra terapeutica che giustificava concentrazioni superiori a 64 µg/mL per i saggi funzionali successivi. I saggi checkerboard hanno rivelato interazioni sinergiche/additive (indici FIC <0,5) con sia ceftazidima sia rifampicina in condizioni standard, riducendo le concentrazioni inibitorie a livelli clinicamente raggiungibili. In particolare, sia Mg^{2+} sia LPS esogeno hanno bloccato completamente l'attività adiuvante del PDSTP, ripristinando l'attività metabolica batterica in tutte le combinazioni.

Il PDSTP ha bloccato l'adesione di PAO1 (riduzione del 70-85% a 50-200 µg/mL), confermando i risultati precedenti. Questo effetto è scomparso completamente con i competitori di LPS ($MgCl_2$, LPS purificato). Tuttavia, su cellule prive di eparan solfato (geneticamente o enzimaticamente trattate), il PDSTP ha continuato a funzionare perfettamente, senza che l'adesione di PAO1 fosse influenzata. La citometria a flusso ha confermato una riduzione di HS >90% nelle cellule A549-610 con knockdown di *B3GAT3* e nelle monocamere trattate con Eparinase III.

Tutti questi esperimenti convergono verso la stessa conclusione: il PDSTP si lega agli LPS di *P. aeruginosa* attraverso i loro gruppi fosfato. Ciò destabilizza l'integrità della membrana esterna, facilitando la penetrazione degli antibiotici e bloccando le interazioni batterio-ospite. Di particolare importanza, le HSPG dell'ospite non risultano coinvolte né nell'adesione di PAO1 né nell'attività di PDSTP.

Questo studio fornisce le evidenze che propongono il PDSTP come un nuovo composto mirato agli LPS, efficace sia come adiuvante antibiotico sia come agente anti-adesione contro *P. aeruginosa* nella FC. Evitando di uccidere direttamente i batteri, il PDSTP minimizza la pressione selettiva per la resistenza, concentrandosi sui passaggi chiave della patogenesi. Questi risultati giustificano validazioni *in vivo* in modelli di FC e studi strutturali delle interazioni PDSTP-LPS per guidare lo sviluppo simile verso la traduzione clinica.

INTRODUCTION

1. Introduction to cystic fibrosis

Cystic fibrosis (CF) is an autosomal recessive disorder caused by mutations in the cystic fibrosis transmembrane conductance regulator (*CFTR*) gene (Ratjen *et al*., 2015). It is a multiorgan condition that primarily affects the respiratory, gastrointestinal, pancreatic, biliary, and reproductive systems (Polgreen and Comellas, 2022). CF is among the most common genetic disorders in Caucasians, with an estimated incidence of 1 in 3,200 live births. However, prevalence differs across ethnic groups: 1 in 13,500 among Hispanic populations, 1 in 15,000 in individuals of African descent, and 1 in 35,000 in Asian populations (Dickinson and Collaco, 2021). In the United States alone, approximately 10 million people are carriers of a CFTR mutation. The implementation of universal newborn and prenatal genetic screening is expected to further increase the number of identified carriers. Consequently, there is a growing research interest in the lifetime health risks associated with the CF carrier state (Polgreen and Comellas, 2022). According to the Italian Cystic Fibrosis Research Foundation (FFC Ricerca), approximately 6,000 individuals are affected in Italy, 48,000 across Europe, and 160,000 worldwide (https://www.fibrosicisticaricerca.com/the-foundation-ffc/).

1.1. Genetic basis of CF

The underlying cause of the disease are mutations in the CFTR gene, which encodes a protein responsible for the transport of anions across the cell membrane (Radlović, 2012). The CFTR gene was cloned by Riordan *et al.* in 1989 and is located on the long arm of chromosome 7 (7q31.2). It spans approximately 250 kilobases and contains 27 exons. Thanks to this knowledge, modern DNA analysis is a valuable tool in both prenatal and postnatal diagnostics of the disease, as well as in identifying its heterozygous carriers (Radlović, 2012).

To date, more than 2,000 CFTR mutations have been identified (http://www.genet.sickkids.on.ca/cftr/), of which over 360 are disease-causing variants (www.cftr2.org). These findings have led to the functional classification of CFTR variants into seven major classes, as illustrated in **Fig. 1** (Lee *et al.*, 2021).

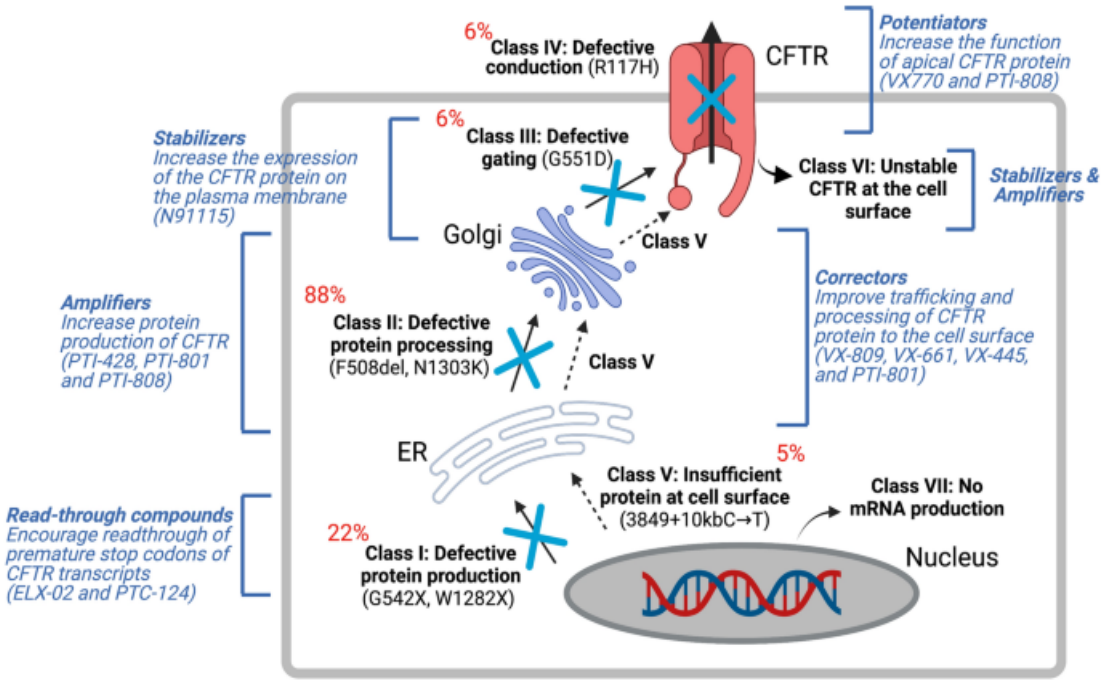

Figure 1. *Classes and prevalence of CFTR variants and their impact on CFTR expression and processing. For each defect a proper CFTR modulator therapy is described (Lee et al., 2021).*

The seven classes of CFTR mutations are distinguished based on the resulting protein defect. Class I mutations affect protein production that result in a complete absence of functional CFTR protein; 22% of patients carry at least one of these mutations. Class II mutations impair protein processing and trafficking, causing CFTR misfolding and reduced expression at the plasma membrane. This category is the most common, with about 88% of patients carrying at least one mutant allele; the Phe508del (F508del) variant represents the prototypical defect. Class III mutations involve defective channel gating, preventing proper opening of the ion channel, and occur in roughly 6% of affected individuals. Class IV mutations alter ion conductance through the channel and are found in approximately 6% of cases. Class V mutations reduce the overall amount of protein synthesized, thereby limiting the number of functional channels at the cell surface; these defects are estimated to affect about 5% of patients. Class VI mutations, in turn, destabilize CFTR at the plasma membrane, accelerating its removal and degradation, and are present in around 5% of cases. Lastly, Class VII mutations interfere with CFTR transcription, resulting in the complete absence of mRNA and protein; large deletions, such as CFTRdele2,3 (21 kb), are typical examples of this category (Lee *et al*., 2021).

1.2. CFTR structure and function

The CFTR protein is a 1,480-amino-acid glycoprotein belonging to the adenosine triphosphate (ATP)-binding cassette (ABC) transporter superfamily. Its complex structure allows chloride (Cl^-) ions to cross epithelial cells barrier (**Fig. 2**; Hanssens *et al.*, 2021).

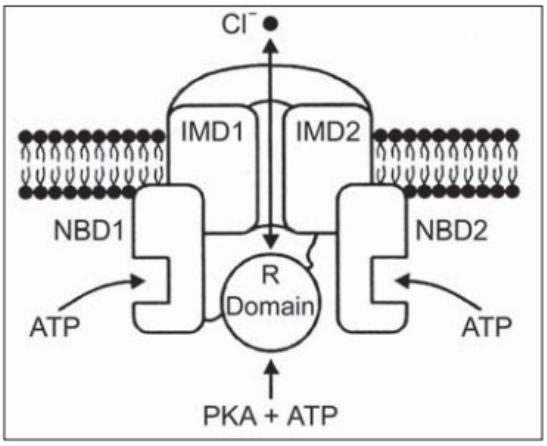

Figure 2. *Schematic presentation of CFTR protein structure and function. IMD – intramembranous domains; NBD – nucleotide-binding domain; R – regulatory (domain); PKA – cAMP-dependent protein kinase (Radlović, 2012).*

CFTR comprises two transmembrane domains (IMD1 and IMD2), two cytosolic nucleotide-binding domains (NBD1 and NBD2), and a regulatory (R) domain. IMDs form the ion channel pore, while gating is controlled by ATP binding and hydrolysis at the NBDs. Channel activation requires ATP binding, which promotes NBD dimerization and chloride efflux. This is followed by ATP hydrolysis, which induces dimer separation and channel closure (Hanssens *et al*., 2021).

1.3. Pathophysiology of CF

Defective CFTR-mediated chloride transport leads to increased sodium absorption and osmotic water reuptake from epithelial surfaces. This causes the mucus to become thicker and more viscous, resulting in mucus plugging and organs obstruction. The most frequently affected organs include the sinuses, lungs, pancreas, hepatobiliary system, intestines, and sweat glands (Sankari and Sharma, 2025). According to the European Cystic Fibrosis Society, respiratory failure was the leading cause of death in 49.12% of cases in 2023 (Zolin A *et al*., 2025), emphasizing the prominent role of lung disease in CF. Indeed, impaired ion transport and mucus obstruction initiate a cascade of pathological events, culminating in chronic inflammation and progressive lung tissue damage. In healthy airways, balanced sodium absorption and chloride secretion maintain the airway surface liquid (ASL) homeostasis and ensure effective mucociliary

clearance, which is the main airways defence mechanism against inhaled pathogens. In contrast, CF airways exhibit mucus stasis and impaired bacterial clearance, favouring persistent colonization. Colonizing microorganisms trigger excessive production of pro-inflammatory cytokines and promote neutrophil recruitment. These cells release proteases and reactive oxygen species (ROS) that directly damage and accelerate lung function decline (**Fig. 3**; Mitri *et al*., 2020).

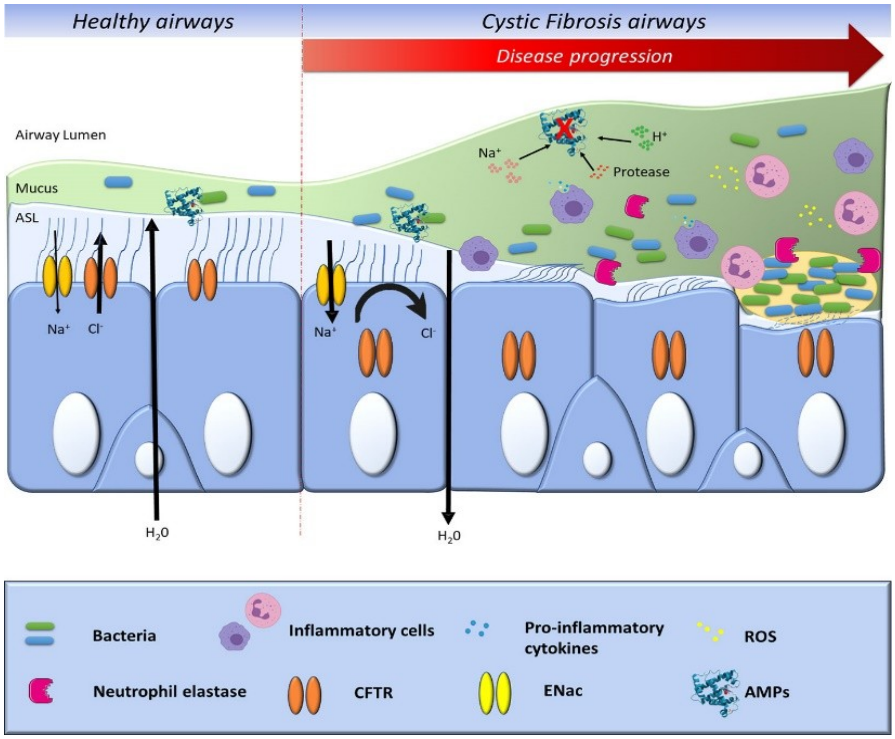

Figure 3. *Graphical representation of CF lung disease progression (Mitri et al., 2020).*

Thick mucus also causes local hypoxia, resulting in sterile inflammation that activates the immune response and the synthesis of interleukins (ILs), especially IL-1α and IL-1β. These are potent proinflammatory molecules that are involved in neutrophilic inflammation, increasing the production of reactive oxygen species, and inhibiting antimicrobial activity in the CF lung. This dysfunctional immune response not only causes hyperinflammation but also predisposes to increased susceptibility to infections that significantly contribute to the progression of lung disease in CF patients (**Fig. 4**; Petrocheilou *et al.*, 2022).

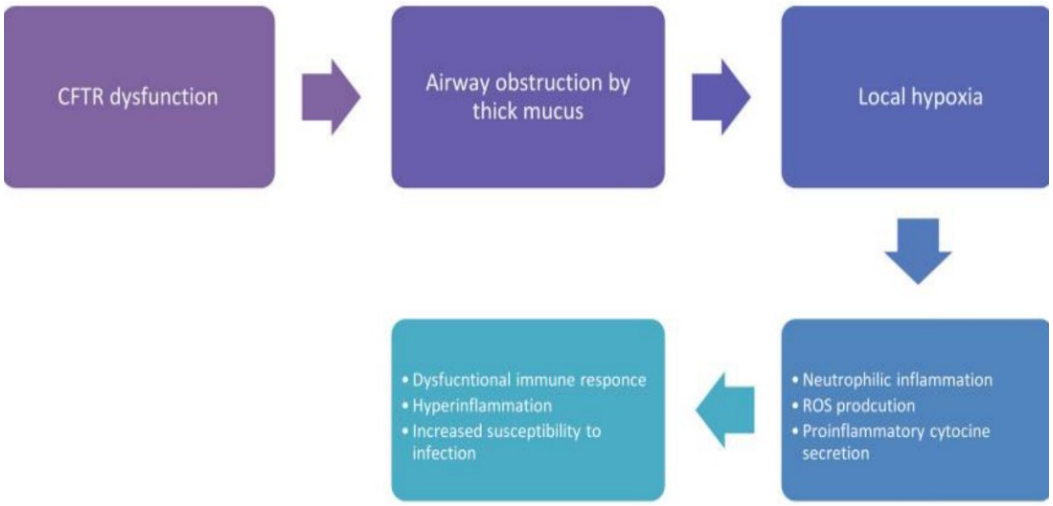

Figure 4. *Correlation between CFTR dysfunction-related inflammation and infection in CF lung (Petrocheilou et al., 2022).*

1.4. Current treatments

Until a few years ago, treatments for CF were only focused on symptom management. Pancreatic insufficiency and intestinal malabsorption were managed through supplementation with pancreatic enzymes, fat-soluble vitamins, and the administration of high-calorie diets. Additionally, therapies aimed at slowing the decline of lung function included physical and inhalation treatments designed to relieve airway obstruction. Antibiotic therapies were also widely used to eradicate bacterial infections. In the advanced stages of the disease, lung transplantation remained the only curative option (Lopes-Pacheco, 2020).

In early 2012, the U.S. Food and Drug Administration approved a new class of drugs known as CFTR modulators (Goetz and Savant, 2021). These are small molecules that bind directly to the CFTR protein with specific affinity during or after its synthesis (Jia and Taylor-Cousar, 2023). CFTR modulators are categorized into five groups based on their effects on mutations: potentiators, correctors, stabilizers, amplifiers, and read-through compounds (**Fig. 1**; Lopes-Pacheco, 2020). Potentiators and correctors are currently clinically available, whereas the other categories remain under development. Potentiators enhance or restore ion channel activity, thereby improving CFTR-mediated chloride and bicarbonate transport. Correctors bind to immature CFTR protein and facilitate its folding and trafficking to the cell membrane. This class of drugs has demonstrated efficacy for specific mutations such as F508del (Jia and Taylor-Cousar, 2023).

Currently, four modulators are commercially available: Ivacaftor, the first approved modulator, is a potentiator (Goetz and Savant, 2021); instead, the other three, Lumacaftor, Tezacaftor, and Elexacaftor, are correctors (Jia and Taylor-Cousar, 2023).
Ivacaftor is administered to patients aged 4 months and older with gating mutations (class III) and has been in use in Europe for over a decade. It binds to the CFTR protein and increases channel opening frequency as well as ion conductance. Lumacaftor was the first CFTR corrector approved, and it is administered in combination with Ivacaftor (LUM/IVA) for patients aged 2 years and older homozygous for the F508del mutation. Several studies suggest that Lumacaftor can correct protein misassembly and improve folding, trafficking, and stability. Tezacaftor is used in combination with Ivacaftor (TEZA-IVA) to treat patients heterozygous for the F508del mutation aged 6 years and older.
Elexacaftor was approved in 2020, entering in clinical practice in combination with Tezacaftor and Ivacaftor (ELX/TEZ/IVA) to further improve conditions of patients homozygous for F508del (Regard *et al*., 2022). Currently, approximately 90% of the CF population carry mutations responsive to CFTR modulators. The remaining 10% continue to rely on symptomatic treatments due to rare mutations or intolerance to modulators caused by side effects (Kramer-Golinkoff *et al*., 2022).

2. Pathogens associated with CF

As previously described, mutations in the *CFTR* gene lead to dysfunctional activity of the CFTR protein, thereby disrupting ion transport across cell membranes (Rumpf *et al*., 2021). This results in the formation of a thick mucus layer on the airway surface of patients, which impairs mucociliary clearance, inhibits the activity of antimicrobial peptides, and promotes bacterial infections (Pang *et al*., 2019).
Individuals with cystic fibrosis (CF) experience chronic lung infections that evolve over time, with the dominant pathogens varying by patient age (**Fig. 5**). Early childhood is typically marked by *Staphylococcus aureus* colonization, followed by a rise in opportunistic Gram-negatives such as *Pseudomonas aeruginosa, Achromobacter* spp., *Stenotrophomonas maltophilia*, and members of the *Burkholderia cepacia* complex (Bcc) during adolescence and adulthood. Although these represent classic CF pathogens, the clinical significance of non-tuberculous mycobacteria, fungi, and viruses is increasingly recognized. These complex and persistent infections are

central to disease progression and represent a major challenge in CF management (Blanchard and Waters, 2019).

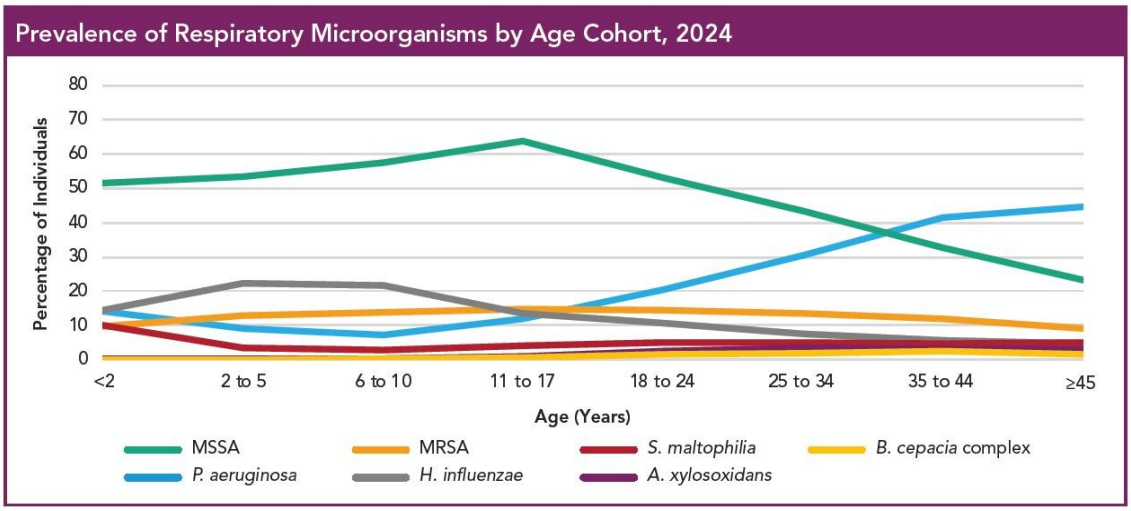

Figure 5. *Age-dependent prevalence of bacterial pathogens in patients with CF (Cystic fibrosis foundation, 2025).*

2.1. *Staphylococcus aureus*

Staphylococcus aureus is a Gram-positive coccus, commonly found as a commensal organism on human skin and mucosal surfaces, especially in the anterior nares and skin creases (**Fig. 6**; Blanchard and Waters, 2019). *S. aureus* is a major pathogen responsible for a wide spectrum of human diseases worldwide. These range from superficial skin infections to severe invasive conditions, such as pneumonia, prosthetic joint infections, endocarditis, and nosocomial bacteraemia (Cheung *et al*., 2021).

In CF, *S. aureus* represents one of the earliest and most prevalent pathogens to colonize the airways, found especially in young children. Its prevalence exceeds 50% before the age of two, peaking around 65% in early adolescence (**Fig. 5**). Long-term colonization of specific clones is observed in many patients (Rumpf *et al*., 2021).

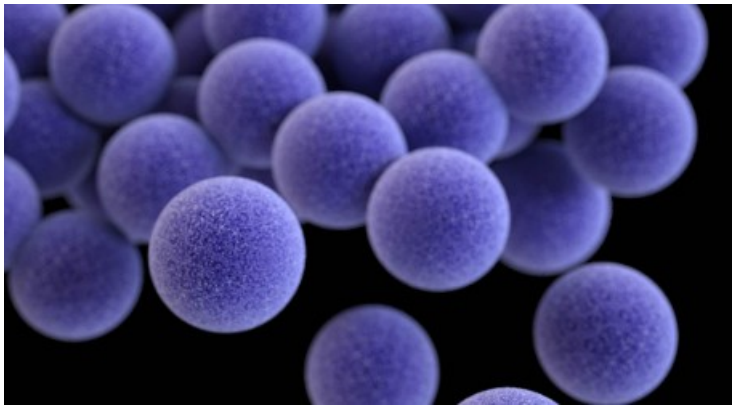

Figure 6. *Coloured scanning electron microscope image of* S. aureus *bacterial cells (Centers for Disease Control and Prevention, 2022).*

The persistence of *S. aureus* in CF airways is promoted by several mechanisms, including the production of diverse virulence factors, the formation of biofilms, and the emergence of antibiotic-resistant strains, such as methicillin-resistant *S. aureus* (MRSA). Biofilms are complex, three-dimensional microbial communities surrounded by an extracellular polymeric substance matrix that protects bacteria from host immune responses and antibiotics. Within biofilms, subpopulations of "persister" cells exhibit transient tolerance to antimicrobial stresses, further complicating eradication efforts.

MRSA arose soon after methicillin's introduction in the 1960s, driven by horizontal gene transfer of the *mecA* gene, which encodes a penicillin-binding protein with low affinity for methicillin and most beta-lactams. Although less prevalent than methicillin-sensitive strains, MRSA affects 10-25% of cystic fibrosis patients worldwide and is associated with accelerated lung function decline and increased mortality (Thornton and Parkins, 2023).

Another important adaptation strategy is the small colony variant (SCV) phenotype, characterized by mutations in metabolic genes that cause reduced growth and increased antibiotic tolerance. SCVs are found in 8-24% of CF patients, especially among those with MRSA infections. Their intracellular localization protects them from many antibiotics, complicating the treatment. Clinically, SCVs correlate with chronic infection, worsened lung function, and frequent coexistence with *Pseudomonas aeruginosa*, representing a key factor in disease progression (Thornton and Parkins, 2023). All these factors make *S. aureus* a major challenge in the clinical management of CF airway infections (Jean-Pierre *et al*., 2022).

2.2. *Stenotrophomonas maltophilia*

Stenotrophomonas maltophilia is an environmental global emerging Gram-negative multidrug-resistant organism (MDRO) most commonly associated with respiratory infections in humans (**Fig. 7**). Also, it causes a variety of other severe infections including bacteraemia and endocarditis (Brooke, 2012). Over the past two decades, *S. maltophilia* has emerged as a significant pathogen in CF patients, and its incidence appears to be on the rise. Regardless of the specific characteristics of the infection, *S. maltophilia* is now recognized as a detrimental pathogen that can have a substantial impact on lung function in individuals with CF (Terlizzi *et al*., 2023).

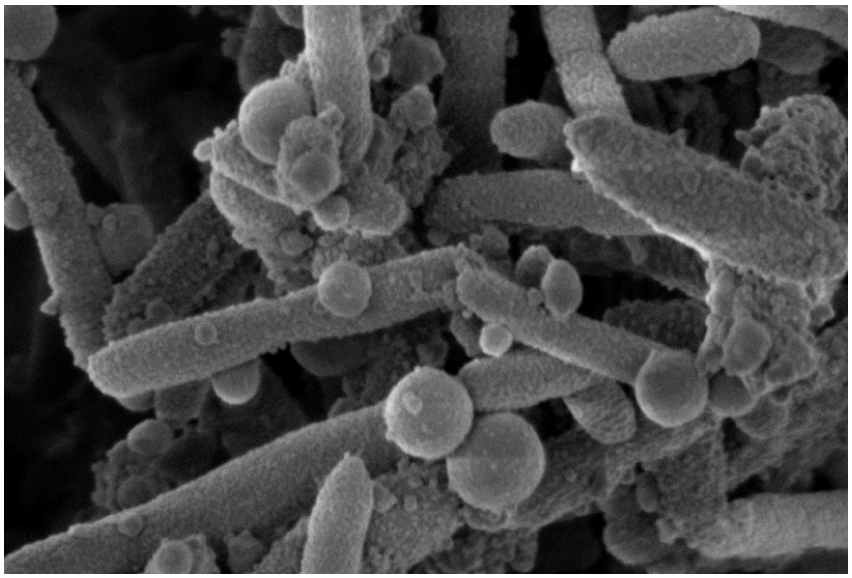

Figure 7. *Scanning electron microscope image of* Stenotrophomonas maltophilia *bacterial cells (German Center for Infection Research, 2020).*

Regarding the prevalence, in 2018 the pathogen has been isolated from the respiratory tracts of 13.8% of people with CF in Canada, 12.3% in the USA and 8.14% in Europe during. This variability may reflect differences in laboratory identification methods (Amin *et al*., 2020). A retrospective case-control study by Denton and Kerr (1998) found an association between the use of anti-pseudomonal antibiotics and isolation of *S. maltophilia* in the respiratory tract. This raises the question of whether aggressive antibiotic treatment targeting *P. aeruginosa* may promote *S. maltophilia* colonization (Amin *et al*., 2020).

Concerning the management of these infections, no consensus guidelines are available and treatments usually rely on fluoroquinolones and combinations of new-generation β-lactams with β-lactamase inhibitors (Amin *et al.,* 2020).

2.3. *Achromobacter xylosoxidans*

Non-fermentative Gram-negative bacilli belonging to the genus *Achromobacter* are recognized as emerging pathogens worldwide in the CF population, with a predominance of the species *Achromobacter xylosoxidans* (**Fig. 8**).

This bacterium can be found in diverse environments, including hospitals, and the prevalence across different CF centres varies widely, ranging from 3 to 30% of CF patients colonized with *A. xylosoxidans*. For example, epidemiological data from the Belgian CF registry in 2013 reported a prevalence of 8.9% in children and 12.2% in adults (Cools *et al*., 2016).

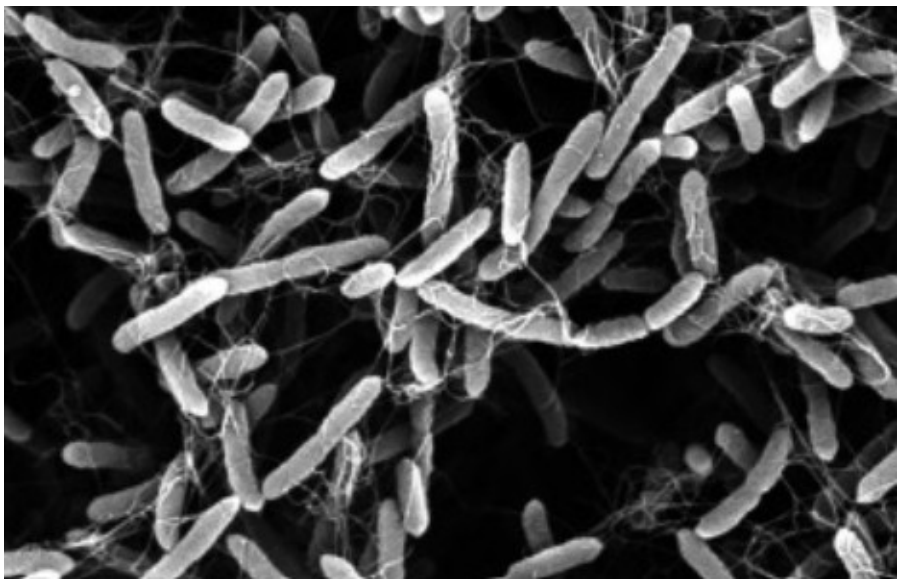

Figure 8. *Scanning electron microscope image of* Achromobacter xylosoxidans *bacterial cells (Sahl et al., 2023).*

While the clinical impact of *P. aeruginosa* and *S. aureus*, particularly MRSA, during colonization and infection of CF patients is well documented, the clinical significance of *A. xylosoxidans* remains a matter of debate. Nonetheless, *A. xylosoxidans* is a well-known opportunistic pathogen implicated in a variety of severe infections including bacteraemia, pneumonia, endocarditis, peritonitis, especially in immunocompromised patients and those with underlying diseases. Moreover, the bacterium may have a role in the decline of CF lung function, since recent studies have shown that it can induce an inflammatory response similar to that caused by *P. aeruginosa* in chronically infected individuals (Menetrey *et al*., 2021).

Similar to *P. aeruginosa*, *Achromobacter* species exhibit several intrinsic characteristics that may explain both their long-term persistence in the lung microbiome and their potential ability to damage lung structure and function. Their highly dynamic genome and hypermutability can favour adaptation to the lung environment and promote colonization or infection. These bacteria possess many virulence factors, including a number of protein secretion systems to deliver lethal toxins into competing bacterial cells. They are resistant to natural antimicrobial peptides present in airway secretions. Finally, they exhibit significant motility, a strong ability to adhere to respiratory epithelial cells and to form biofilms, all key characteristics contributing to persistence, reduced sensitivity to host defences and antibiotic treatment (Esposito *et al*., 2021).

Members of the *Achromobacter* genus are generally multidrug resistant pathogens. This resistance arises from a combination of intrinsic and acquired mechanisms that

frequently work simultaneously to render antibiotics currently used against Gram-negative rods ineffective both *in vitro* and *in vivo*. Efflux mechanisms, beta-lactamase production and mutations in target proteins are key determinants of antibiotic resistance in *Achromobacter* species (Esposito *et al*., 2021).

2.4. Non-tuberculous mycobacteria

Non-tuberculous mycobacteria (NTM) are ubiquitous in the environment and have been isolated from air, soil, dust, plants, natural and drinking water sources, wild animals, milk and food products. NTM cell wall is characterized by a thin peptidoglycan layer surrounded by a thick, lipid-rich outer coating, which facilitates attachment to rough surfaces and confers resistance to antibiotics and disinfectants; this promotes NTM survival under adverse conditions, including low oxygen and carbon availability (**Fig. 9**, Sharma and Upadhyay, 2020).

Figure 9. *Cryo-Scanning electron microscope image of non-tuberculous mycobacteria (Siddam et al., 2021).*

The incidence of NTM infections has been rising in developed countries, largely due to aging populations and an increased prevalence of underlying conditions that predispose individuals to NTM acquisition. A history of chronic lung disease, immunocompromised status, and frequent hospitalization further increase individual risk. People with CF are particularly susceptible to respiratory mycobacteriosis due to bronchiectasis, impaired mucociliary clearance, and repeated antimicrobial treatments.

For this reason, current CF guidelines recommend regular annual NTM screening (Örlős *et al*., 2024).

A new meta-analysis reported an overall NTM prevalence of 7.9% in CF, with significant geographical and age-related variability. National CF patient registries have documented a prevalence of 12% in the United States and France, about 8% in Germany, and below 5% Australia, Brazil and the United Kingdom. In Europe, *Mycobacterium abscessus complex* (MABSC) and *Mycobacterium avium complex* (MAC) are the most frequently detected NTM species in CF patients, with a slight predominance of MABSC (Örlős *et al*., 2024). A recent large multicentre prevalence study in the US has shown that CF patients with NTM-positive sputum cultures tend to be older and have a lower frequency of *P. aeruginosa* pulmonary infection compared to NTM-negative patients. Interestingly, long-term use of azithromycin in CF patients has been associated with increased rates of NTM infection in large UK centres (Hill et al., 2012).

NTM pulmonary disease is associated with accelerated lung function decline and worse clinical outcomes in people with CF, and it is considered a relative contraindication for lung transplantation due to intrinsic resistance to antimicrobial therapy. Consequently, specific guidelines have been implemented for CF patients, outlining evidence-based screening, drug susceptibility testing, and standardized diagnostic criteria. Floto *et al.* (2016) have devised recommendations for screening, investigation, diagnosis, and management of NTM lung infections in people with CF, with evaluation and targeted therapy indicated for patients meeting American Thoracic Society/Infectious Diseases Society of America (ATS/IDSA) criteria and in accordance with the Clinical and Laboratory Standards Institute (CLSI) guidelines (Gramegna *et al.,* 2023).

2.5. *Burkholderia cepacia* complex

Burkholderia cepacia complex (Bcc) is a group of Gram-negative bacteria comprising more than 20 species, including *B. cepacia*, *B. cenocepacia* and *B. multivorans* (**Fig. 10**, Jin *et al,* 2020).

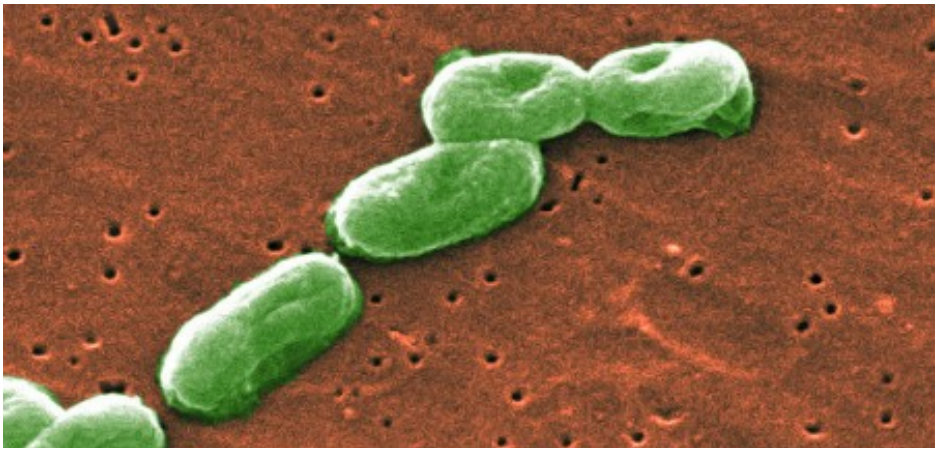

Figure 10. *Coloured scanning electron microscope image of* Burkholderia cepacia *bacterial cells (Centers for Disease Control and Prevention, 2025).*

The species within this genus exhibit high phenotypic diversity and are ubiquitously distributed across diverse ecological niches, including water, soil, industrial environments, artificial products, plants, and invertebrate and vertebrate animals. They also frequently colonize cosmetic, disinfectant, and pharmaceutical products intended for hospital use (Gutiérrez and Coria, 2024).

Bcc bacteria have been reported as opportunistic pathogens that cause pneumonia in people with CF or chronic granulomatous disease. These organisms are associated with accelerated decline in pulmonary functions, increased morbidity and mortality, and reduced survival following lung transplantation. Patients infected with Bcc bacteria can develop cepacia syndrome, a severe clinical condition characterized by necrotizing pneumonia and sepsis, with very high mortality risk (Jin *et al.,* 2020).

In recent years, the incidence of Bcc infections in Europe in children ranges around 1-5%, while it is up to 18% in adults (Zolin *et al*., 2025). Until the 2000s, *B. cenocepacia* was the most prevalent Bcc species causing lung infections in CF, but, in the last 15 years, an increase in the proportion of *B. multivorans* has been reported in many countries. However, a high prevalence of *B. cenocepacia* infections has persisted in certain populations, such as Czech and Italian populations (Drevinek and Mahenthiralingam, 2010).

The management of Bcc microorganisms' infections is particularly challenging due to their production of a wide variety of virulence factors and their innate resistance to many antibiotics and disinfectants. Indeed, these bacteria can adhere to epithelial cells and mucin, invade and survive inside airway epithelial cells and macrophages, and form biofilms that protect them from host defences and antibiotics treatments. They possess a peculiar lipopolysaccharide structure that is implicated in antibiotic and antimicrobial

peptide resistance and secrete factors such as catalases, proteases and siderophores that help evade host defences and survive in hostile environments (Lord *et al.,* 2020).
Therefore, infection with Bcc species remains a significant concern in the CF population due to the associated morbidity and mortality (Blanchard and Waters, 2019).

3. Pseudomonas aeruginosa

Pseudomonas aeruginosa is a ubiquitous Gram-negative bacterium belonging to the family Pseudomonadaceae (**Fig. 11**; Pang *et al.*, 2019). It is a facultative anaerobic microorganism that colonizes various habitats, including soil, surface waters, rivers, oceans, and wastewater treatment plants (Lund-Palau *et al.,* 2016).

Figure 11. *Coloured scanning electron microscope image of the bacterium* Pseudomonas aeruginosa *(Centers for Disease Control and Prevention, 2019).*

P. aeruginosa represents a major nosocomial threat, especially within intensive care environments where it contributes to elevated mortality in patients with pneumonia, chronic obstructive pulmonary disease (COPD), and CF lung disease (Liao *et al.,* 2022). As a member of the multidrug-resistant "ESKAPE" group (*Enterococcus faecium*, *Staphylococcus aureus*, *Klebsiella pneumoniae*, *Acinetobacter baumannii*, *Pseudomonas aeruginosa* and *Enterobacter species*) known for their increasing prevalence of drug resistance and bacterial virulence, the World Health Organization designated *P. aeruginosa* as a top antibiotic-resistant "priority pathogen" urgently requiring new treatments (Liao *et al.,* 2022).

The remarkable adaptability of *P. aeruginosa* to natural and anthropogenic environments is granted by its relatively large genome, ranging from 5.5 to 7 Mbp, compared to other sequenced bacteria. It encodes a high proportion of regulatory enzymes involved in metabolism, transportation and the efflux of organic compounds, providing an enhanced coding capability that allows for great metabolic versatility and high adaptability to environmental changes. The genomic and metabolic versatility enables *P. aeruginosa* to rapidly adapt to hostile environments, including the respiratory tract of CF patients, which is characterized by chronic inflammation, hypoxic zones and high concentrations of antibiotics. The outer membrane (OM), which is an exclusive feature of Gram-negatives, confers additional protection from environmental stresses to the bacterium. OM constitutes the outer part of the cell envelope and is organized as an asymmetric bilayer, with phospholipids on the inner leaflet and lipopolysaccharides on the outer one (**Fig. 12**, Huszczynski *et al.,* 2019).

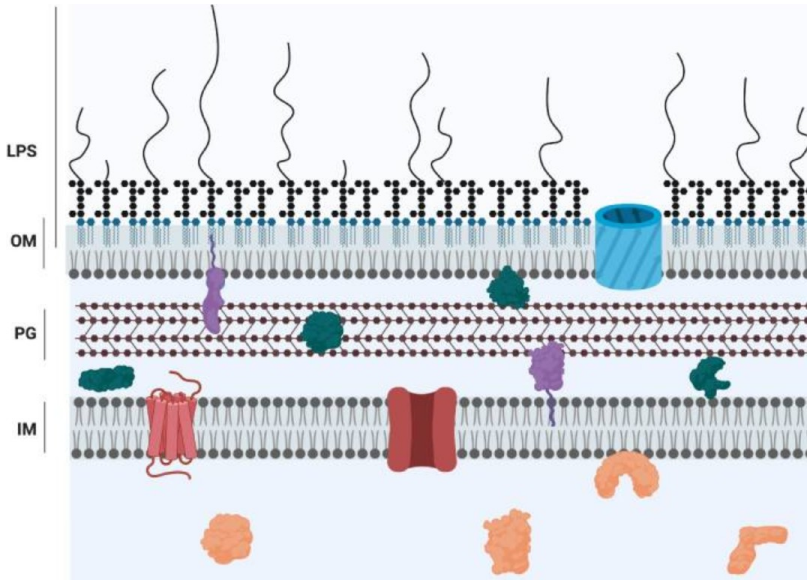

Figure 12. *Representation of the Gram-negative cell envelope. The outer membrane (OM) is an asymmetric bilayer containing phospholipids and lipopolysaccharides (LPS), while the inner membrane (IM) is symmetric with phospholipids. The periplasmic space between them contains a thin peptidoglycan (PG) layer (Huszczynski et al., 2019).*

P. aeruginosa's adaptability enhances its resistance to treatments and allows it to establish chronic infections in CF airways, also thanks to the expression of several virulence factors (Pang *et al.*, 2019, Ambreetha *et al.,* 2024).

3.1. *P. aeruginosa* recognition and adhesion to respiratory epithelial cells

P. aeruginosa is rarely pathogenic for healthy individuals' lung, thanks to the intact airway epithelial barrier and immune defences; the development of infection depends

largely on epithelial injury, mucociliary clearance dysfunction, or immune system impairment. Acute or chronic pneumonia usually affect immunocompromised patients or those with impaired pulmonary function, such as individuals with CF (Muggeo *et al.,* 2023).

The intact human airway epithelium (HAE) serves as both physical and functional barrier against pathogens. This pseudostratified, differentiated mucociliary bronchial epithelium is composed of multiple specialised cells types supported by the underlying basement membrane. In healthy epithelium, only the apical membrane is exposed to the environment. Injuries, varying from disruptions of tight junctions to partial epithelial shedding, or even complete denudation of the basement membrane, trigger a repair process aimed at regenerating and restoring epithelial function. In chronic inflammatory respiratory diseases, such as CF, dysregulated inflammation impairs this repair process (Muggeo *et al.,* 2023).

The HAE's barrier function relies on intercellular junctions, especially tight junctions, which maintain epithelial polarity and impermeability. A hallmark of *P. aeruginosa* infections is the exploitation of breaches in this barrier to access basolateral receptors, normally concealed by tight junctions. Exposure of basolateral surface is essential for the initiation of respiratory infections by *P. aeruginosa* (Muggeo *et al.,* 2023). Respiratory infections begin with *P. aeruginosa* adhering to airway epithelial cells or to the basement membrane. Surface appendages such as pili, and flagella serve as virulence factors responsible for motility and attachment. Through diverse motility mechanisms (swarming, swimming, and twitching), *P. aeruginosa* senses and colonizes suitable surfaces for adhesion. Several host molecules, particularly glycoconjugates with long carbohydrate chains on epithelial and extracellular matrix components, are involved in bacterial adhesions (**Fig. 13**; Muggeo *et al.,* 2023).

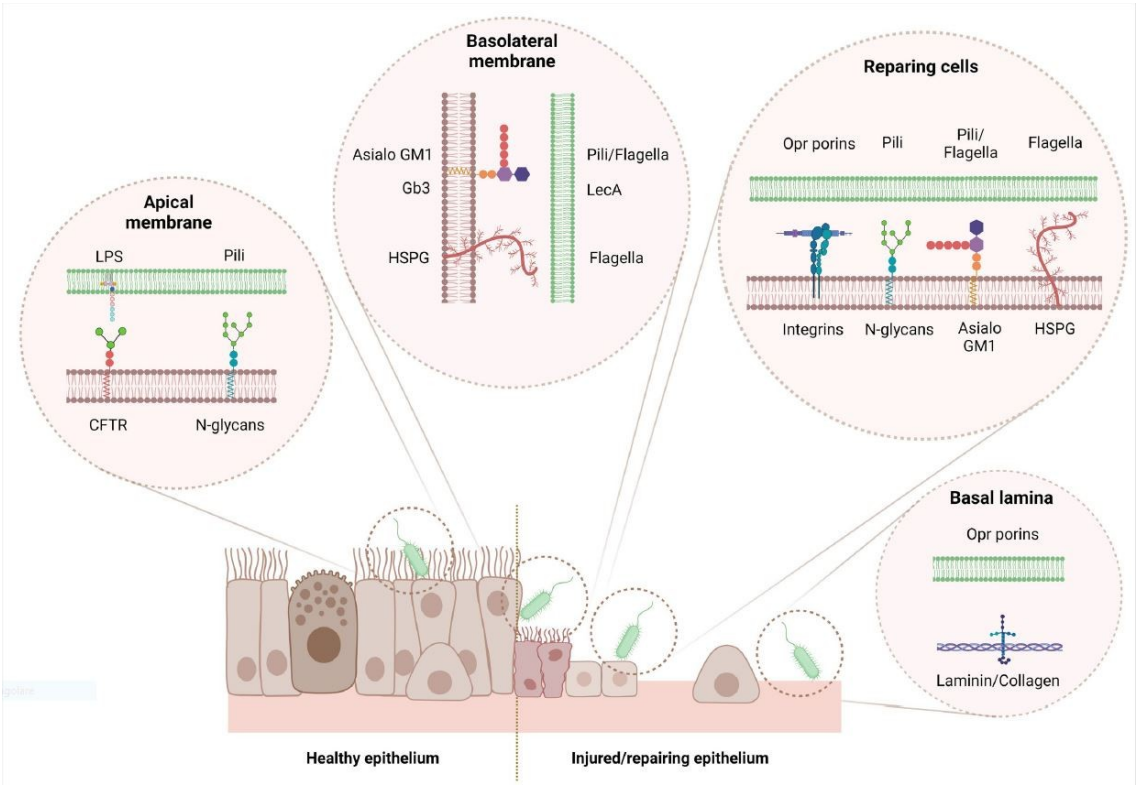

Figure 13. *Airway receptors of* P. aeruginosa *(Muggeo et al., 2023).*

The distribution of host receptors varies depending on tissue condition. At the apical surface of healthy epithelium, receptor expression is limited, restricting bacterial interaction. However, heparan sulfate proteoglycans, primarily localised at the basolateral surface, are aberrantly expressed at the apical surface in regenerating or CF epithelia. This creates a permissive environment for bacterial attachment and persistent colonization (Muggeo *et al.,* 2023). In particular, *P. aeruginosa* flagellum mediates maximal binding to heparan sulfate chains at the basolateral surface, triggering activation of the epidermal growth factor receptor, adaptor protein Shc, and the PI3K/Akt pathway, resulting in bacterial internalization. Conversely, type IV pili bind host N-glycans on the apical surface, similarly activating the PI3K/Akt pathway and facilitating bacterial entry (Bucior *et al.,* 2012).

3.1.1. Heparan sulfate proteoglycans as receptors for *P. aeruginosa* adhesion

Heparan sulfate proteoglycans (HSPGs) belong to a subclass of proteoglycans that are located at the plasma membrane and within the extracellular matrix of human cells, acting as major modulators of cell adhesion, tissue architecture, and receptor-mediated signaling (Sarrazin *et al.,* 2011; García *et al.,* 2016).

Structurally, HSPGs consist of a core protein covalently linked to one or more heparan sulfate (HS) glycosaminoglycan (GAG) chains. The considerable diversity in the number and length of HS chains, as well as their further modification by various sulfation patterns (at N, 2, 3, and/or 6 positions), underlies the enormous structural and functional heterogeneity of these molecules (**Fig. 14**; Bucior *et al*., 2010).

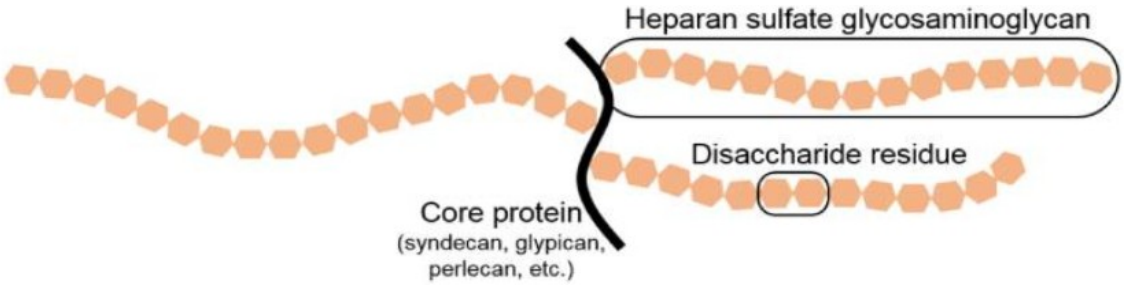

Figure 14. *General structure of HSPGs (Egorova et al., 2021).*

There are three main classes of HSPGs, defined by their cellular location: membrane-associated HSPGs (such as syndecans and glypicans), secreted extracellular matrix HSPGs (including agrin, perlecan, and type XVIII collagen), and the secretory vesicle proteoglycan serglycin. Due to their highly anionic nature, conferred by abundant sulfated HS chains, HSPGs display high structural diversity and are able to bind a wide variety of ligands (Sarrazin *et al,* 2011).

The first step in the establishment of *P. aeruginosa* infection is the receptor-mediated binding to the injured epithelium, such as the CF lung epithelium, specifically at the apical (AP) and/or basolateral (BL) surfaces. Glycoconjugates, including glycolipids, glycosylated proteins, and proteoglycans, serve as receptors for *P. aeruginosa* binding, as their long carbohydrate chains are displayed on the cell surface (Bucior *et al*., 2010).

Among these, HSPGs are preferentially expressed on the BL surface of polarized epithelia and may serve as key BL receptors for *P. aeruginosa*. Experimental and *in vitro* studies have established that the HS chains of HSPGs are necessary and sufficient to mediate bacterial binding, invasion, and cytotoxicity at the BL surface in polarized cells, with the degree of sulfation being a critical determinant of this interaction (Bucior *et al*., 2010). However, although sulfation is a critical determinant of *P. aeruginosa* binding and cytotoxicity, the significance and precise contribution of specific HS modifications in bacterial pathogenesis remain largely unknown (Aquino *et al.,* 2018; Bucior *et al*., 2010).

Flagella and type IV pili represent the predominant *P. aeruginosa* adhesins, mediating initial host recognition and attachment. Bucior and colleagues (2012) demonstrated that flagella are essential for HSPGs recognition and binding, gaining an insight into our comprehension of the intricate *P. aeruginosa*-epithelial cells interactions.

HSPGs not only serve as critical receptors mediating *P. aeruginosa* adhesion and invasion of respiratory epithelial cells, but also represent promising therapeutic targets. Disrupting the interaction between bacterial adhesins and host HSPGs has gained increasing attention as an antivirulence strategy aimed at preventing infection establishment and biofilm formation. Such approaches have the potential to reduce antibiotic resistance and improve clinical outcomes by targeting bacterial virulence without exerting selective pressure for resistance development (Bucior *et al*., 2010; Sarrazin *et al,* 2011).

3.2. Virulence factors

P. aeruginosa produces a wide variety of virulence factors, which can be grouped into cell-associated and extracellular components. Cell-associated virulence factors include surface structures such as lipopolysaccharides (LPS), flagella, pili and outer membrane proteins that facilitate initial adhesion and colonization of host tissues. In addition, *P. aeruginosa* possesses multiple secretion systems that deliver extracellular factors, including secreted toxins, enzymes and signalling molecules, into host cells, contributing to tissue damage, immune evasion and bacterial persistence. Furthermore, quorum-sensing and biofilm formation mechanisms enable bacterial communication, long-term persistence and resistance to antimicrobial treatments (**Fig. 15**; Liao *et al.,* 2022).

Thanks to its broad repertoire of virulence factors and notable adaptability, *P. aeruginosa* is the most prevalent pathogen in CF lung infections, establishing persistent colonization that resists treatment in the harsh CF airways environment (Jurado-Martín *et al.,* 2021).

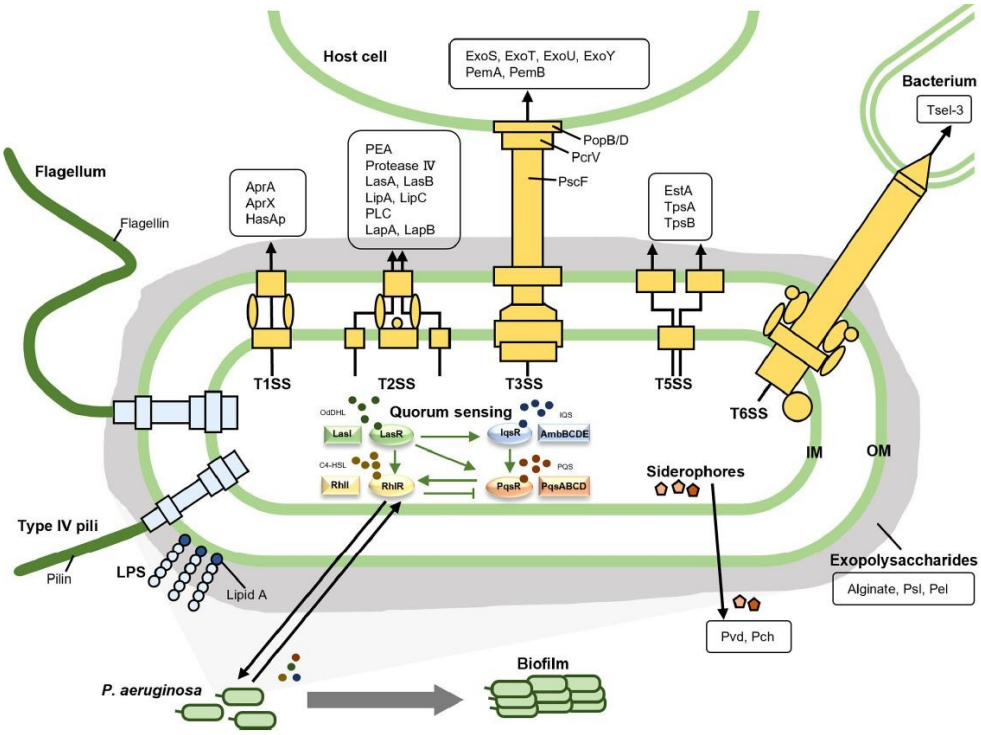

Figure 15. *Overview of the main virulence factors of* Pseudomonas aeruginosa*, grouped into surface structures, secreted factors, and cell-to-cell interaction mechanisms (Liao et al., 2022).*

3.2.1. Lipopolysaccharides

Lipopolysaccharides **(**LPS) are major virulence factors of *P. aeruginosa*, forming the principal component of the outer leaflet of the outer membrane in Gram-negative bacteria. These complex glycolipids serve both as a physical barrier, protecting the bacterium from host immune responses and antibiotics, and as mediators of direct interactions with host cell receptors (King *et al.,* 2009).

Structurally, LPS are composed of three distinct domains: lipid A, core oligosaccharide, and O-antigen (also known as O polysaccharide; **Fig. 16**).

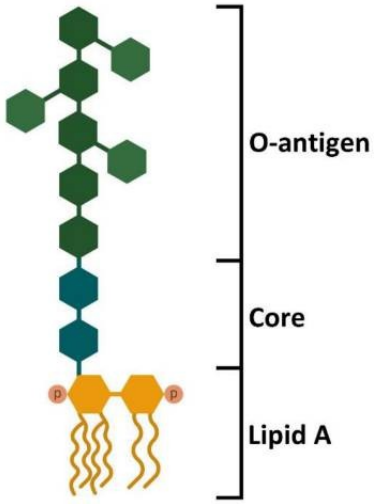

Figure 16. *structure of LPS (Galgano et al., 2022).*

Most *P. aeruginosa* strains produce two different forms of O-antigen, which contribute to immunogenic diversity and strain classification. The most common O-antigen contains a homopolymer of D-rhamnose, while the other form is a heteropolymer with three to five distinct sugars in its repeat units (Lam *et al.,* 2011). The O-antigen is highly immunogenic, and elicits a strong antibody response from the infected host. In chronic *P. aeruginosa* infections, it is common for strains to reduce O-antigen production and then to lose it altogether. These changes may be driven by the selective pressures on the bacteria to evade the anti-O-antigen immune response. Another selective pressure for loss of O-antigen may be exposure of the bacteria to repeated antibiotic therapy (King *et al.,* 2009).

LPS are amphipathic molecules that significantly reduce membrane permeability in Gram-negative bacteria: the hydrophobic lipid A impedes the passage of polar solutes, while the polar O-antigen and core oligosaccharides repel lipophilic compounds (Huszczynski *et al.,* 2019).

In addition to their structural roles, LPS mediate interactions with host receptors, and induce tissue damage through their endotoxic activity. Additionally, LPS induce reactive oxygen species (ROS) production and mucin overproduction in airway epithelial cells, worsening disease severity in asthma and CF patients. They also enhance antibiotic resistance by promoting outer membrane vesicles (OMVs) production and biofilm maturation, enabling long-term bacterial persistence (Jurado-Martín *et al.,* 2021).

3.2.2. Adhesins and pili

P. aeruginosa employs a variety of adhesins and pili to initiate host colonization and establish infection. These components mediate initial attachment, motility and biofilm formation, which are critical steps in establishing infection. Among the principal adhesins, there are the flagellins FliC and FliD, which form the flagellar filament and the cap structure, respectively, and type IV pili (T4P; Jurado-Martín *et al.,* 2021).

P. aeruginosa motility depends on a polar flagellum consisting of a helical FliC flagellin filament, FliD cap protein, FlgE hook, two FlgKL junction proteins, and basal body components spanning both outer and inner membranes. This structure is responsible for swimming motility in liquid or low viscosity environments and chemotaxis, while also enabling initial binding to the CF airway epithelia (Jurado-Martín *et al.,* 2021). Aside from motility, FliC interacts with host glycans (including heparan sulphate proteoglycans) to promote early attachment and biofilm formation, while FliD mediates adhesion to human respiratory MUC1 mucin (Jurado-Martín *et al.,* 2021).

Bacterial motility and virulence often depend on surface appendages called pili, highly flexible protein-based filaments extending from the cell envelope (Jacobsen *et al.,* 2020). Multiple pili variants have been classified according to their structure and assembly mechanism.

In *P. aeruginosa*, Type IV pili (T4P) enable key virulence functions such as twitching motility, DNA uptake, and host cell adhesion. T4P comprises type IVa pili (T4aP) and type IVb pili (T4bP), with T4bP driving biofilm formation, colonization and adhesion (Jacobsen *et al.,* 2020). These pili consist of abundant PilA major pilin subunits plus less abundant tip-positioned minor pilins, classified as core minor pilins (pili formation and tip stabilisation) and non-core minor pilins (aggregation, adhesion and DNA uptake) (Jurado-Martín *et al.,* 2021).

3.2.3. Secretion systems

Among virulence factors, secretion systems and their transported effectors play a crucial role, with the Type III Secretion System (T3SS) being the most relevant in *P. aeruginosa* pathogenesis. T3SS facilitates bacterial colonisation, survival and replication by injecting effector proteins into host cells. These effectors disrupt host immune defences by actively manipulating host cellular processes, including actin

cytoskeletal organization and signal transduction pathways and promoting bacterial colonisation and survival (Horna and Ruiz, 2021).

Four well characterised toxic effectors are secreted via T3SS: ExoU, ExoT, ExoS, and ExoY. Two novel effectors have been proposed (PemA and PemB), along with other proteins such as flagellar and Pilus proteins. ExoU, a potent phospholipase A2, is considered the primary cytotoxin due to its greatest impact on disease severity and association with severe acute lung injury, sepsis, and mortality. It irreversibly destroys host cell membrane, causing rapid cell death. (Jurado-Martín *et al.,* 2021).

ExoY, the second most prevalent exotoxin, is a soluble adenylate cyclase that increases intracellular cyclic nucleotides levels in host cells, activating protein kinases. As a result, it triggers irreversible actin microtubule disassembly, cell death via necrosis, and endothelial barrier breakdown, ultimately leading to lung damage and multi-organ failure (Jurado-Martín *et al.,* 2021).

3.2.4. Siderophores

Siderophores are low molecular weight iron chelating molecules secreted by bacteria to scavenge ferric iron (Fe^{3+}) from the environment and deliver it back into the cell via specific uptake systems, thus satisfying an essential nutritional requirement in iron limited niches such as the airways (Minandri *et al.,* 2016). *P. aeruginosa* produces two siderophores, pyoverdine and pyochelin, which display very different structural and functional properties. Pyoverdine, a peptide siderophore featuring two hydroxamate groups and a fluorescent dihydroxyquinoline moiety, forms a highly efficient iron-chelating complex. In contrast, pyochelin, a salicylate-type siderophore, exhibits lower iron affinity (Minandri *et al.,* 2016).

Pyoverdine also functions as a signalling molecule that regulates the expression of multiple virulence factors, including exotoxin A and specific proteases, and is considered a key virulence determinant in lung infection models (Minandri *et al.,* 2016).

In CF lungs, iron availability is altered by chronic inflammation and tissue damage, and *P. aeruginosa* exploits siderophore production together with additional iron-uptake systems to establish and maintain long term infection (Konings *et al.,* 2013). For these reasons, siderophore biosynthesis and uptake systems are being explored as potential targets for novel anti virulence strategies against *P. aeruginosa* infections.

3.2.5. Quorum sensing

Quorum sensing (QS) is a bacterial cell-cell communication process that regulates gene expression in response to changes in cell population density. *P. aeruginosa* possesses four main quorum sensing systems, LasI-LasR, RhlI-RhlR, PQS-MvfR and Iqs, which are interconnected in a hierarchical regulatory network (**Fig. 17**; Tuon *et al*., 2022).

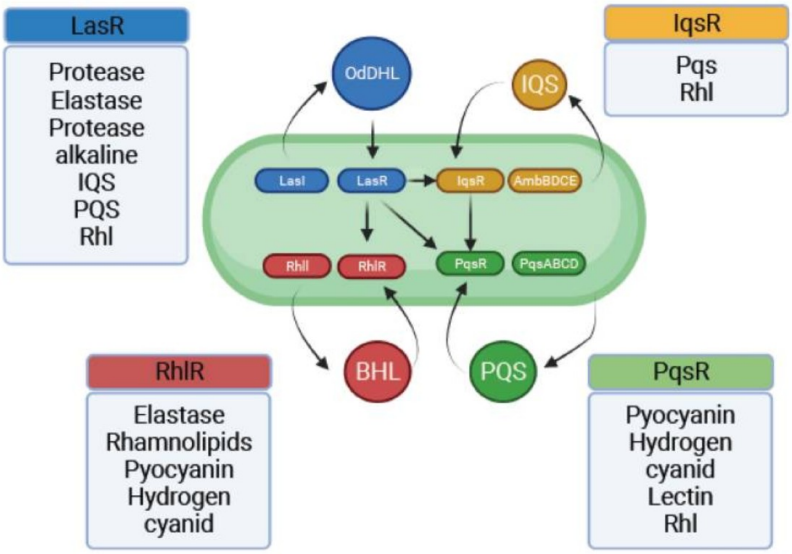

Figure 17. *Genes of the quorum sensing systems of Pseudomonas aeruginosa with regulatory looping and molecules associated with biofilms and pathogenicity (Tuon et al., 2022).*

QS involves the production, secretion and accumulation of signalling molecules called autoinducers (AI), whose specificity and concentration are sensed by specific transcriptional regulators, resulting in the expression or repression of defined sets of genes on a population-wide scale. In addition to biofilm development, QS has been linked to the regulation of other physiological processes, including virulence-factor production (pyocyanin, elastase and rhamnolipids), stress tolerance, metabolic adjustment and host-microbe interactions. In the context of CF lung infection, QS contributes to the establishment and maintenance of chronic *P. aeruginosa* infections by promoting biofilm formation, immune evasion and persistence within antibiotic-tolerant biofilms, as well as tolerance to host-derived stresses. Thus, understanding and controlling these chemical communication systems could lead to new targets for alternative or complementary treatments to conventional antimicrobials and antibiotics (Thi *et al.,* 2020).

Particularly, recent findings show that the QS network in *P. aeruginosa* is highly adaptable and capable of responding to external biotic and abiotic stresses, as seen in chronic CF isolates where alternative pathways compensate for frequent LasR dysfunction, which provides the pathogen with flexibility in the control of virulence gene expression (Bjarnsholt *et al.,* 2010). This is an important factor to consider in the development of quorum sensing inhibitors (QSIs) as therapeutics, since bacteria routinely encounter adverse environmental conditions and selective pressures within the CF lung, which may favour the emergence of resistant mutants (Lee and Zhang, 2015).

3.3. Current therapies against *P. aeruginosa* CF lung infections

Current therapies for *P. aeruginosa* lung infections in people with CF are largely based on prolonged and repeated antibiotic regimens, including both inhaled and systemic formulations (Alqasmi, 2024). Inhaled antibiotics such as tobramycin, colistin, aztreonam lysine and levofloxacin are widely used for chronic suppressive therapy, often administered in alternating on-off cycles (Li and Schneider-Futschik, 2023). Systemic antibiotics, including intravenous or oral agents such as ceftazidime, piperacillin-tazobactam, meropenem and ciprofloxacin, are mainly employed during pulmonary exacerbations or for early eradication attempts (Langton and Smyth, 2017). However, intrinsic, acquired and adaptive resistance mechanisms, together with biofilm-mediated tolerance, progressively reduce the efficacy of these regimens and limit long-term infection control (Elfadadny *et al.,* 2024).

3.4. Mechanisms of antibiotic resistance

3.4.1. Porins

The outer membrane of Gram-negative bacteria constitutes a semipermeable barrier that slows the penetration of antibiotics and other harmful molecules. Nevertheless, *P. aeruginosa* must allow nutrients to enter the cell; this is accomplished through a series of water-filled protein channels known as porins. Genomic sequence analysis of *P. aeruginosa* has identified 163 outer membrane proteins (OMP), 64 of which are grouped into three porin families. These play an essential physiological role in the transport of sugars, amino acids, phosphates, divalent cations, and siderophores (Lister *et al.,* 2009). Typical porin proteins are composed of a 16-strand transmembrane β-

barrel structure, comprised of seven short-turn sequences on the periplasmic side which act as hinges connecting eight external loop structures (Li *et al.,* 2012).

Carbapenems, including imipenem and meropenem are frequently used to treat *P. aeruginosa* infections. To date, three carbapenem resistance mechanisms have been identified including reduced carbapenem influx due to changes in the expression of outer membrane porin OprD, production of carbapenemases and efflux pump overexpression. In particular, defective OprD expression is among the most common resistance mechanism found in carbapenem-resistant *P. aeruginosa* strains (Lister *et al.,* 2009).

3.4.2. Lipopolysaccharide (LPS) modifications

Lipopolysaccharides (LPS) form the outer leaflet of the Gram-negative outer membrane, creating a highly impermeable barrier that restricts antibiotic entry while allowing nutrient passage. In *P. aeruginosa*, LPS consists of lipid A anchored in the membrane, a core oligosaccharide, and a variable O-antigen polysaccharide that contributes to surface diversity and immune evasion (Pang *et al.,* 2019). Lipid A, the hydrophobic anchor and endotoxic component, is normally negatively charged due to phosphate groups, facilitating binding of cationic antibiotics like colistin. Resistance arises primarily through chemical modifications of lipid A that neutralize its negative charge, reducing colistin binding. The most common mechanisms involve addition of 4-amino-4-deoxy-L-arabinose (L-Ara4N) to the 4'-phosphate, mediated by the ArnT transferase encoded in the *arnBCADTEF-oprG* operon, or phosphoethanolamine (PEtN) to the 1-phosphate via EptA transferase (*eptA* gene). These modifications are regulated by two-component systems: PmrAB (ParRS in some strains) senses low Mg^{2+} or cationic peptides activating *arn* expression, while PhoPQ responds to environmental cues for *eptA* (Moskowitz *et al.,* 2004; Cervoni *et al.,* 2023). Such adaptations confer high-level colistin resistance in CF isolates and are often co-selected with other resistance traits (Cervoni *et al.,* 2023).

3.4.3. Multidrug efflux pumps

Multidrug efflux pumps are integral membrane protein complexes that actively export antibiotics and toxic compounds from the bacterial cytoplasm or periplasm, contributing to intrinsic and inducible multidrug resistance in *P. aeruginosa*. These systems belong

primarily to the Resistance-Nodulation-Division (RND) superfamily, forming tripartite assemblies spanning the inner membrane (IM), periplasm, and outer membrane (OM): an IM pump (e.g., MexB), a periplasmic adaptor (MexA), and an OM channel (OprM) (Pang *et al.,* 2019). *P. aeruginosa* expresses at least five major RND efflux systems with overlapping yet distinct substrate specificities: MexAB-OprM (constitutively expressed, expels β-lactams, fluoroquinolones, macrolides), MexXY-OprM (inducible by aminoglycosides, targets tobramycin/gentamicin), MexCD-OprJ (inducible, broad-spectrum including chloramphenicol), MexEF-OprN (substrates include carbapenems/macrolides), and MexJK-OprM (naturally repressed). Expression is tightly regulated by repressor proteins (e.g., MexR, NalC, NalD for MexAB-OprM) that, when mutated or inactivated, lead to overexpression and resistance (Pang *et al.,* 2019; Lorusso *et al.,* 2022). These pumps synergize with porin loss and enzymatic inactivation, driving multidrug resistance phenotypes prevalent in CF chronic infections (Tomás *et al.,* 2010).

3.4.4. Enzymatic inactivation

Enzymatic inactivation represents a primary resistance mechanism in *P. aeruginosa*, whereby specialized enzymes hydrolyze, phosphorylate, or acetylate antibiotics, rendering them inactive (Torrens *et al.,* 2019). This occurs in the periplasm (β-lactamases) or cytoplasm (aminoglycoside-modifying enzymes, AMEs), preventing drug-target interaction. The chromosomal *ampC* gene encodes AmpC cephalosporinase, a class C β-lactamase that hydrolyzes penicillins, cephalosporins (ceftazidime), but not carbapenems or monobactams. *ampC* expression is inducible by β-lactams via the LysR-type regulator AmpR, which senses cell wall-derived muropeptides; mutations in *ampR*, *dacB* (PBP4), or peptidoglycan recycling genes lead to stable iper-production in clinical isolates (Torrens *et al.,* 2019). Aminoglycosides (tobramycin) are inactivated by AMEs: AAC(6')-Ib acetylates, ANT(2")-I adenylates, and APH(3') nucleotidylates/transfers phosphate, often plasmid-mediated and co-selected with efflux (Vaziri *et al.,* 2011). These mechanisms synergize with porin loss/efflux, driving multidrug resistance in chronic CF infections (Pang *et al.,* 2019; Tomás *et al.,* 2010).

3.4.5. Biofilm formation and the appearance of persister cells

Isolation of persistent strains from chronic infections reveals mechanisms that allow *P. aeruginosa* to adopt a biofilm-associated lifestyle, which confers tolerance to antibiotic treatment and aids in evasion of the host immune response (Gheorghita *et al.,* 2023).

It has been estimated that biofilms have a substantial bearing on over 90% of chronic infections. For this reason, it is important to diagnose *P. aeruginosa* infections at an early stage, before biofilm development, which could enhance the susceptibility of *P. aeruginosa* towards antimicrobial treatments (Thi *et al.,* 2020).

A biofilm is a highly structured community of bacterial cells encased in a self-produced matrix of extracellular polymeric substances. The matrix of the biofilm is composed of extracellular DNA (eDNA) (<1%), RNA (<1%), proteins (<2%), exopolysaccharides (1–2%), water (97%). The matrix, which is responsible for more than 90% of biofilm biomass, acts as a scaffold for adhesion to biotic and abiotic surfaces and shelter for encased bacteria; it also facilitates cell-to-cell communication (Thi *et al.,* 2020; Gheorghita *et al.,* 2023). *P. aeruginosa* is genetically capable of producing three biofilm exopolysaccharides: alginate, Pel, and Psl, each of which has a role in chronic infections and confers advantages to the bacterium against eradication (Gheorghita *et al.,* 2023). Pel is a cationic polysaccharide polymer involved in the initiation of surface attachment, as well as maintenance of biofilm integrity. Psl is a neutral pentasaccharide necessary for adhesion of sessile cells (cells attached to a surface) to surfaces and cell-to-cell interactions during biofilm initiation of both non mucoid and mucoid strains (Thi *et al.,* 2020). Alginate is predominately produced in the biofilm of mucoid *Pseudomonas* strains. The mucoid phenotypes are found mostly in CF isolates, signifying the conversion from acute to chronic infection. Alginate is a negatively charged acetylated polymer necessary for biofilm maturation, protection from phagocytosis and opsonization, and decreased diffusion of antibiotics through the biofilm (Thi *et al.,* 2020). Alginate attaches to mucin found in the respiratory tract, acting as an adhesin, and its acetyl groups increase the viscosity, which accumulate water and nutrients in the biofilm (Tuon *et al*., 2022).

Biofilm development is divided into five distinct stages and it is mainly controlled by QS. Stage I: Bacterial cells adhere to a surface via support of cell appendages such as flagella and type IV pili; this adherence is reversible. Stage II: Bacterial cells undergo the switch from reversible to irreversible attachment. Stage III: Progressive propagation

of attached bacteria into a more structured architecture, together with the formation of microcolonies. Stage IV: Microcolonies develop further into extensive three-dimensional mushroom-like structures, a hallmark of biofilm maturation. Stage V: In the center of the microcolony, matrix cavity is disrupted through cell autolysis for the liberation of dispersed cells followed by the transition from sessile to planktonic growth mode for seeding of uncolonized spaces (Stage VI), which allows the biofilm cycle to restart (Thi *et al.,* 2020).

Within the biofilm, a subpopulation of cells adopts a persister-like phenotype characterized by low metabolic activity and dormancy. These cells are responsible for the high antibiotic tolerance of biofilm-associated infections, including the ones in CF lung (Borisova *et al.,* 2025).

3.5. Alternative therapies

Multidrug-resistant *P. aeruginosa* constitutes a major global health threat. Its acquisition of resistance genes has severely reduced therapeutic options for life-threatening infections, increased disease burden, and increased mortality rates due to failed treatments, necessitating coordinated worldwide antimicrobial resistance surveillance. This looming health threat, together with a limited progress in new antibiotics development, has restimulated interest in the development of new antimicrobial therapies (De Oliveira *et al.,* 2020). Combination antibiotic regimens with adjuvants, bacteriophage therapy, antimicrobial peptides, nanoparticles, and immunotherapy represent extensively studied alternatives (Mulani *et al.,* 2019).

Therapies targeting bacterial virulence represent an additional valid approach to combat the rise of antimicrobial resistance by focusing on neutralizing the key pathogenic mechanisms rather than directly killing the bacteria or inhibiting their growth. Such antivirulence strategies aim to reduce bacterial infectivity by blocking virulence factors critical for disease progression, thereby reducing the selective pressure for drug resistance development (Liao *et al.,* 2022).

3.5.1. Bacteriophage therapy

One promising alternative that is being explored to treat antimicrobial resistant bacterial infections, especially in CF lung disease, is bacteriophage therapy. Phages are century old therapeutic agents historically used for the treatment of bacterial infections. They

possess several characteristics that make them ideal candidates for clinical use. First, they have high specificity towards their bacterial targets, minimizing disruption to the human microbiome. Second, they are generally well tolerated by individuals receiving therapy. Third, they are highly abundant in the environment and they are efficacious against antimicrobial resistant bacteria. Unlike antibiotics, phages have the ability to co-evolve with their bacterial hosts, developing new infectivity mechanisms as bacteria mutate (Canning *et al.,* 2024; Mulani *et al.*, 2019).

Several *in vitro* studies have demonstrated the effectiveness of phages against both biofilm-associated and planktonic cells of *P. aeruginosa* (Jennes *et al*., 2017; Duplessis *et al*., 2018). Despite their promise, phage therapy presents some limitations. The high specificity of phages, though advantageous, can be restrictive. Monophage therapy requires *in vitro* evaluation of phage efficacy against the specific pathogenic strain before clinical application, which can be a difficult process. The use of phage cocktails combinations of phages targeting different bacterial species or strains can help overcome this issue, although their practical implementation in clinical settings remains challenging (Mulani *et al.*, 2019).

Phage lysogeny can result in the acquisition of resistance or virulence genes by host bacteria. Moreover, the subsequent lysis of bacterial cells possessing phage-encoded virulence factors can result in the release and horizontal transfer of these genes to other bacteria. Thus, genomic characterization of phages is essential to ensure their safety for therapeutic use. Therapeutic phages should therefore be screened to ensure they lack such genes, as well as integrases, site-specific recombinases, or repressors of the lytic cycle that may facilitate gene integration into the bacterial genome (Mulani *et al.*, 2019).

Another important limitation involves phage formulation stability and delivery to infection sites. Administration routes include oral, nasal, and topical, with nebulization being particularly relevant for CF lung infections.

To overcome some of these limitations, phage therapy can be combined with antibiotics, potentially producing synergistic effects that enhance the efficacy of one or both agents. Such combinations have been reported to reduce bacterial biofilm formation. However, the success of phage antibiotic combination therapy remains uncertain, as the underlying mechanisms of synergy are not yet fully understood and *in vivo* evidence is limited. Further research is required to draw definitive conclusions (Mulani *et al.*, 2019).

3.5.2. Antimicrobial peptides

Antimicrobial treatments improve survival of CF patients, but the high salt concentrations, the acidic pH and the presence of many biomolecules in the viscous mucus reduce antibiotic efficacy. Antimicrobial peptides (AMPs) have emerged as promising alternative candidates due to low toxicity, reduced antibiotic resistance development, and anti-inflammatory effects (Bugli *et al.,* 2022). AMPs are short positively charged oligopeptides of the innate immune system, produced across taxa from protozoa to mammals. They exhibit a broad spectrum of activities against a wide range of pathogens, including *P. aeruginosa* (Mulani *et al.*, 2019).

AMPs interact electrostatically with bacterial membranes, causing lysis and providing advantages against multidrug-resistant (MDR) strains. In contrast to conventional antibiotics, AMPs mechanism of action makes it difficult for bacteria to develop resistance against them (Mulani *et al.*, 2019).

Inhalation is the preferred administration route for drug targeting respiratory dysfunction in CF, including AMPs, enabling direct lung delivery while minimizing off-target effects compared to oral routes. The respiratory tract facilitates peptide administration through: 1) a large surface area for near-simultaneous drug exposure, unlike the intestine; 2) high blood flow avoiding direct hepatic metabolism; 3) relatively low metabolic activity (Bugli *et al.,* 2022).

While preclinical studies demonstrate promising efficacy (Chen *et al*., 2017), further research is essential to optimize AMP stability and activity through designing synthetic derivatives with advanced delivery systems, and to address mucus penetration challenges for effective inhalation therapies against biofilm-associated infections (Bugli *et al.,* 2022).

3.5.3. New therapies based on CRISPR/Cas system

Among innovative strategies against *P. aeruginosa* CF infections, the CRISPR (clustered regularly interspaced short palindromic repeats)/Cas system has received significant attention due to its high specificity. Currently, no direct CRISPR-based anti-infective treatments exist clinically (Qian *et al.,* 2023).

The CRISPR-Cas system, comprising CRISPR sequences and Cas proteins, functions as an adaptive immune mechanism in bacteria and archaea against foreign nucleic acids. Within the last decade, it has become the most efficient and convenient gene

editing tool. CRISPR-Cas system can be also exploited to develop new therapies against drug-resistant bacteria. There are two main categories: pathogen-centered approaches, targeting essential chromosomal regions, and gene-centered strategies, eliminating resistance plasmids. For example, CRISPR interference has identified the chromosomal gene *fprB*, encoding a ferredoxin $NADP^+$ reductase, essential for *P. aeruginosa* survival during oxidative stress, as a promising target to disrupt biofilms in CF infections (Zhang *et al.,* 2025)

Tailored targeting can selectively eliminate strains or reduce resistance gene abundance in microbial communities, depending on infection dynamics (Qian *et al.,* 2023). This therapy faces various challenges in terms of safety (off-target cleavage causing cytotoxicity), delivery across CF mucus barriers, editing efficiency in bacteria and regulatory approval. CRISPR-Cas technology is also being investigated for diagnosing ESKAPE infections through collateral cleavage detection platforms (Qian *et al.,* 2023).

3.5.4. Immunotherapy

Immunotherapy represents a promising strategy to combat *P. aeruginosa* infections in CF, by enhancing host immune responses or neutralizing key virulence factors. Monoclonal antibodies (mAbs) derived from B cells of CF patients targeting *P. aeruginosa* PcrV, a type III secretion system component, demonstrated potent protection in murine pneumonia models, reducing bacterial burden without inducing antibiotic resistance (Hale *et al.,* 2025).

Anti-bacterial antibodies bind bacterial cells or neutralize toxins, stimulate opsonophagocytic killing by phagocytes, promote complement deposition, and facilitate pathogen clearance (Horspool *et al.,* 2023). Immunization strategies against *P. aeruginosa* have mainly focused on major antigens such as LPS, flagellar proteins, and outer membrane proteins F and I (OprF/I). LPS O-antigen-based vaccines elicit protective antibodies in animal models, but protection is serotype-specific (Sousa *et al.,* 2021).

In CF, colonizing *P. aeruginosa* strains are typically flagellated (serotype “a” or “b”); vaccination with *P. aeruginosa* flagella conferred protection in animal models and produced statistically significant infection reduction in CF patients versus placebo (Sousa *et al.,* 2021). Outer membrane proteins (OMPs) are surface-exposed, conserved, and immunogenic, making them attractive vaccine candidates. The most extensively

studied OMPs are the major porin F (OprF) and the lipoprotein I (OprI); an OprF/I vaccine has been shown to induce opsonic antibodies and antibodies that interfere with IFN-γ binding to *P. aeruginosa* (Sousa *et al.,* 2021). This OprF/I vaccine shows promising results as an active vaccine, and new formulations combining it with Th17-stimulating antigens such as type III secretion protein PopB are under investigation to enhance mucosal protection (Sousa *et al.,* 2021).

However, single-antigen vaccines often provide limited protection. Multivalent formulations incorporating multiple *P. aeruginosa* antigens show enhanced immune responses and preventive potential (Sousa *et al.,* 2021). Further understanding of *P. aeruginosa* molecular pathogenesis in CF lungs is still required for the development of novel vaccines and immunotherapies against chronic infections.

3.5.5. Antimicrobial nanoparticles

Nanomedicine exploits metal nanoparticles, such as silver nanoparticles (AgNPs), to combat infections caused by drug-resistant *P. aeruginosa* strains. AgNPs, synthesized via physical, chemical, or biological methods, exhibit potent antibacterial activity through silver ions (Ag^{+}) release which disrupt electron transport, signal transduction and generate reactive oxygen species (ROS) damaging cell walls, membranes, DNA, and proteins (Mulani *et al.*, 2019). AgNPs effectively target both planktonic cells and biofilms of MDR bacteria, a critical feature for chronic CF lung infections. Although sub-inhibitory AgNP exposure risks resistance development, antibiotic combinations enhance efficacy, reduce doses, and minimize toxicity (Mulani *et al.*, 2019).

Current literature highlights a lack of comprehensive *in vivo* studies evaluating the toxicity, efficacy, pharmacokinetics, and immunomodulatory effects of AgNPs. Therefore, further well-designed preclinical and clinical trials are necessary to advance the safe and effective application of antimicrobial nanoparticles in combating resistant infections (Mulani *et al.*, 2019).

3.5.6. Drug repurposing

The research and pre-clinical stages of conventional drug discovery are expensive, time-consuming, and bear high failure rates due to toxicity and safety issues. Drug repurposing (or repositioning) addresses these challenges by utilizing FDA-approved

drugs with established safety profiles, significantly reducing development timelines and costs (Aggarwal *et al.,* 2024).

This strategy proves particularly valuable against multidrug-resistant ESKAPE pathogens. Combination therapies of antibiotics with repurposed drugs having antibiotic adjuvant effect enhance efficacy through synergistic mechanisms, mitigate resistance development, broaden antimicrobial spectra, and lower antibiotic dosages (Aggarwal *et al.,* 2024).

In CF, high-throughput screening under CF-mimicking conditions identified ebselen, carmofur, and tirapazamine as promising candidates that disrupt *P. aeruginosa* membranes, increasing permeability and inducing cell death (Di Bonaventura *et al.,* 2023). Additionally, glatiramer acetate, approved for multiple sclerosis, synergizes with tobramycin against *P. aeruginosa* CF respiratory isolates, reducing MICs even in resistant strains (Murphy *et al.,* 2022).

Bibliometric data show growing interest in drug repositioning for infectious diseases. In the face of increasing MDR strains, combination therapy may prove to be the most effective solution to antibiotic resistance (Glajzner *et al.,* 2024). However, research is needed to ensure that repurposed drugs reach their target sites while limiting side effects and maintaining antimicrobial activity. Drug interactions between synergistic combinations and medications for concomitant diseases pose additional challenges, potentially accelerating resistance (Glajzner *et al.,* 2024).

Rigorous preclinical and clinical studies remain essential to identify viable repositioning candidates. Nevertheless, antibacterial therapy using repurposed drugs against multidrug-resistant infections holds substantial therapeutic and commercial potential (Glajzner *et al.,* 2024).

Overall, these alternative therapeutic strategies offer promising results to combat MDR *P. aeruginosa*, especially in the contexts of CF. While significant progress has been made in preclinical and early clinical research, continued investigations are essential to optimize efficacy, safety, and delivery methods. These innovations hold the potential to complement or even replace traditional antibiotics, addressing the urgent need for effective treatments against MDR infections and improving patient outcomes.

4. Dispirotripiperazines and PDSTP compound

Dispirotripiperazines are molecules with a peculiar chemical structure composed of three cycles with two shared nitrogen atoms (dispiro compounds). They can be classified into three types, based on the cycles composition: 1) Piperazines, systems with three six-membered cycles; 2) Homopiperazines, systems with two six-membered cycles and one seven-membered cycle; 3) Systems with one six-membered cycle and two seven-membered cycles. These molecules possess high antiviral potential that has been unveiled through the study of the most promising dispirotripiperazine derivatives (Egorova *et al*., 2021). Among them, PDSTP, short for: 3,3'-(2-methyl-5-nitropyrimidine-4,6-diyl)3,12-bis-6,9-diaza-diazoniadispiro [5.2.5.2] hexadecane tetrachloride dihydrochloride, is the best characterized compound, possessing excellent metabolic stability, negligible cytotoxicity and a broad-spectrum of efficacy *in vitro* and *in vivo* against viruses using HSPGs as receptors, including herpes simplex virus and Sars-CoV-2 (Alimbarova *et al*., 2022; Sanna *et al*., 2025). PDSTP possesses four quaternary positively charged nitrogen atoms (**Fig. 18**), which are essential for its biological activity, mediating its high affinity for HSPGs. In fact, PDSTP antiviral mechanism of action relies on the saturation of HSPGs on mammalian cells surface, blocking viral recognition and entry of the host cell.

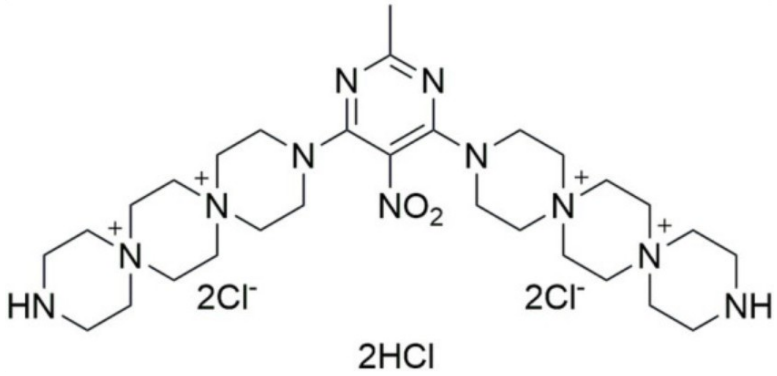

Figure 18. *Chemical structure of the compound PDSTP (Bonacorsi et al., 2024).*

4.1. Antivirulence and antibiotic adjuvant effects of PDSTP against *P. aeruginosa*

Host cell recognition and adhesion is a fundamental step also for bacterial pathogenesis, particularly for the ones colonizing epithelia, as in the case of CF. Since many bacteria use HSPGs as initial receptors for host-pathogen interactions (García *et al*., 2016), including *P. aeruginosa*, PDSTP was repurposed as inhibitor of bacterial adhesion.

In our laboratory, PDSTP was demonstrated to possesses a promising anti-adhesion activity, by using adhesion assays on monolayers of immortalized human epithelial respiratory cells. Specifically, *P. aeruginosa* PAO1 adhesion to A549 cell monolayers was reduced up to 95.9% in the presence of 400 µg/mL PDSTP with an already significant reduction of 41.4% at 10 µg/mL (**Fig. 19**; Bonacorsi *et al*., 2024).

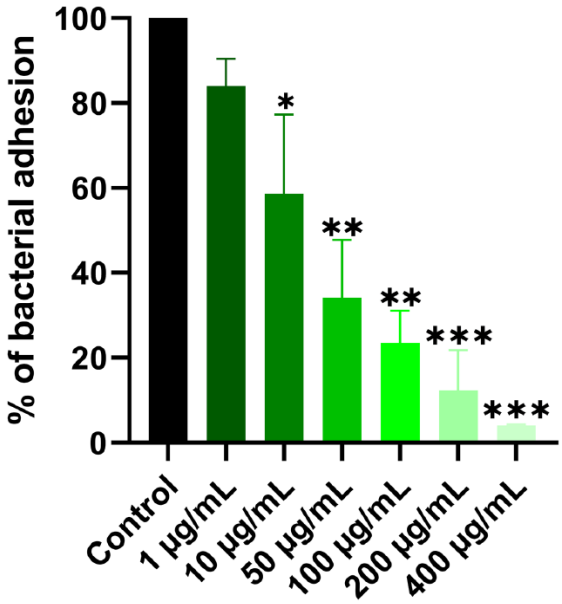

Figure 19. *Adhesion of* Pseudomonas aeruginosa *PAO1 on A549 cell monolayers in the presence of increasing concentrations of PDSTP (Bonacorsi et al., 2024).*

Imaging flow cytometry further confirmed these results (**Fig. 20**; Bonacorsi *et al*., 2024), illustrating PDSTP's capacity to disrupt early colonization of the epithelium.

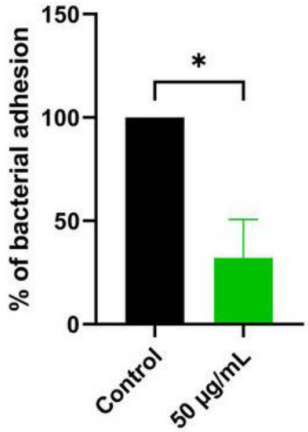

Figure 20. *Adhesion of GFP-expressing* Pseudomonas aeruginosa *PAO1 on A549 cell monolayers without treatment or in the presence of 50 µg/mL of PDSTP (Bonacorsi et al., 2024).*

Furthermore, in the same study, PDSTP showed also an unexpected additional effect on *P. aeruginosa* virulence, strongly inhibiting biofilm formation at concentrations as low as 50 µg/mL; this was shown using confocal laser scanning microscopy (CLSM) and measuring the biofilm biomass decrease in the presence of the compound (**Fig. 21**; Bonacorsi *et al.,* 2024).

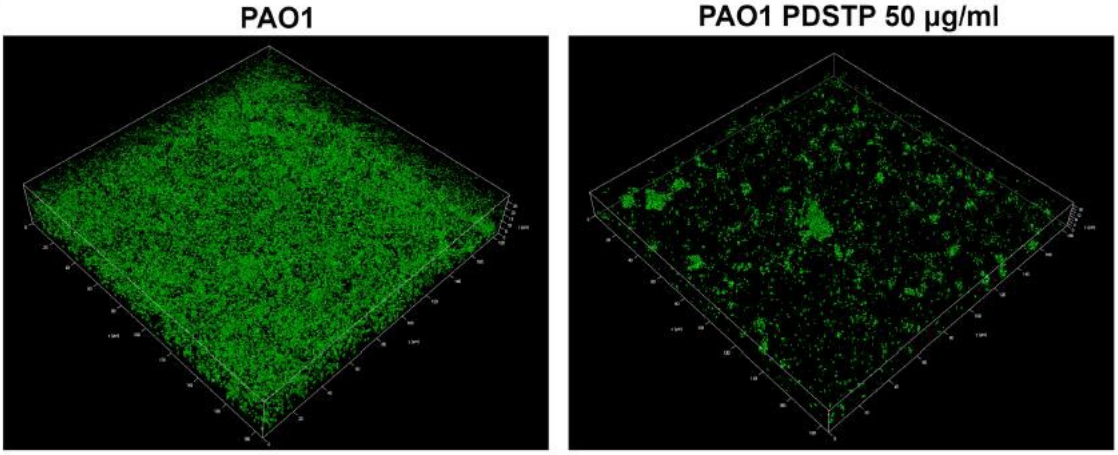

Figure 21. *CLSM images (400x magnification) of* Pseudomonas aeruginosa *biofilms formed with or without PDSTP treatment (Bonacorsi et al., 2024).*

Finally, beyond anti-adhesion and anti-biofilm effects, PDSTP was shown to potentiate conventional antibiotic efficacy against MDR *P. aeruginosa* CF isolates. The compound enhanced antibacterial activity of diverse antibiotics, such as tobramycin, colistin, ciprofloxacin, meropenem and ceftazidime (Bonacorsi *et al.,* 2024). Notably, when combined with ceftazidime, PDSTP reduced the minimum inhibitory concentration (MIC) by up to 128-fold, restoring antibiotic efficacy against resistant strains and being effective also *in vivo* in a *Galleria mellonella* model of infection (Bonacorsi *et al.,* 2024).

Altogether, these findings pose PDSTP as a promising candidate for the development of a novel anti-pseudomonal treatment combining different activities, that include anti-adhesion, anti-biofilm and antibiotic adjuvant effects.

In this study, PDSTP mechanism of action was not investigated but, since its chemical properties make it unable to cross biological membranes, it is expected to involve interactions with molecules on bacterial and mammalian cell surfaces.

It is known that, for its antiviral activity, PDSTP primarily targets HSPGs on respiratory epithelial cells, where its quaternary positively charged nitrogen atoms engage electrostatic interactions with the sulfate groups of HSPGs, effectively blocking

adhesion. It is likely that this mechanism is also important for anti-bacterial adhesion but we cannot exclude that a PDSTP-bacterium interaction may be involved in this process.

Regarding its antibiotic adjuvant mechanism, PDSTP is hypothesized to electrostatically interact with negatively charged molecules localized on the *P. aeruginosa* outer membrane, probably LPS. Our theory is that this interaction would impair the outer membrane barrier, facilitating antibiotic influx. Although these speculations require further investigation, the dual targeting of both HSPGs and LPS highlights PDSTP's multifaceted biological activities and underlines the complexity of its interactions with eukaryotic and prokaryotic cells.

AIM OF THE WORK

Antimicrobial resistance has significantly reduced the efficacy of standard antibiotic therapies, especially against opportunistic Gram-negative pathogens such as *Pseudomonas aeruginosa*, which is a major cause of chronic lung infections in people with cystic fibrosis. In this context, new compounds that are able to enhance antibiotic activity and interfere with bacterial adhesion and colonization of host tissues represent a promising complementary strategy to conventional treatments. PDSTP, a dispirotripiperazine derivative, has recently emerged as a candidate molecule able to potentiate the efficacy of different antibiotics and to reduce *P. aeruginosa* adhesion to lung epithelial cells, potentially preventing lung colonization, and suggesting a dual role as antibiotic adjuvant and anti-adhesion agent. However, although the anti-pseudomonal potential is evident, there is still a lack of information about the mechanism of action of this compound. The high molecular weight and polarity of PDSTP make it unable cross biological membranes, thus we hypothesize that, in bacteria, it may have a target localized on the cell surface. Considering the net positive charge of PDSTP, due to the presence of reactive quaternary nitrogen atoms, we speculate that the compound could interact with negatively charged phosphates of lipopolysaccharide (LPS), the most abundant molecule on Gram-negative outer membrane, with a fundamental role in membrane stability. Regarding PDSTP interaction with mammalian cells, it is known that heparan sulfate (HS) are critically involved in PDSTP antiviral effect but their role in anti-bacterial adhesion is still unclear. Moreover, PDSTP toxicity on epithelial cells has never been investigated.

For these reasons, the aim of this thesis was to elucidate all these aspects by investigating safety and mechanism of action mediating PDSTP antibiotic adjuvant and anti-adhesion activities against *P. aeruginosa* PAO1. First, the cytotoxicity of PDSTP towards human A549 lung epithelial cells was assessed by MTT assay, in order to identify non-toxic concentration ranges suitable for further *in vitro* and *in vivo* preclinical testing. Then, to unveil the putative role of *P. aeruginosa* surface LPS in PDSTP antibiotic adjuvant activity, checkerboard assays were used to evaluate the efficacy of PDSTP combinations with different antibiotics in the presence or absence of an excess of Mg^{2+} ions or purified exogenous LPS, used as competitors of PDSTP binding. The same approach was used to investigate the possible contribution of LPS-PDSTP interactions in mediating the anti-adhesion effect; adhesion assays using A549

cell monolayers were carried out in the presence of an excess of the same PDSTP binding competitors. Additionally, through RNA interference, a mutant A549 cell line not expressing HS was prepared by Prof. Peviani's research group, and the decrease in HS expression was analysed by immunofluorescence. This cell line was used to perform adhesion assays in order to assess the role of HS in PDSTP anti-adhesion activity. Lastly, these results were confirmed by repeating the same experiment using A549 cell monolayers after the treatment with heparinase III, an enzyme that specifically cleaves surface HS.

MATERIALS AND METHODS

Bacterial strains

Strain	Characteristics	Source
Pseudomonas aeruginosa PAO1	Clinical isolate derived strain	Laboratory collection

Pseudomonas aeruginosa PAO1

P. aeruginosa PAO1 is a reference strain widely used for studies on this opportunistic Gram-negative pathogen. It derives from the original PAO isolate obtained in Australia in 1954 and is characterized by intrinsic resistance to several antibiotics. PAO1 is considered a standard laboratory model for investigating bacterial pathogenicity, intrinsic and acquired antibiotic resistance, and for evaluating novel antimicrobial and adjuvant compounds *in vitro* (Grace *et al.,* 2022).

Human immortalized cell lines

The adenocarcinoma lung epithelial cell line **A549** is a human cell line widely exploited as *in vitro* model to study respiratory infections and host response. Three A549-derived cell lines, specifically engineered for heparan sulfate modulation, were generated via HIV-based lentiviral transduction using the pLKO.1 vector (https://www.addgene.org/8453/) and generated by Prof. Peviani's research group (University of Pavia).

- **A549-SCR** (scramble control): transduced with non-targeting shRNA (random sequence) that does not silence any specific gene, serving as the negative control with normal heparan sulfate surface expression (verified by flow cytometry, see results).
- **A549-609**: engineered with *B3GAT3*-targeting shRNA that provides ineffective knockdown, maintaining heparan sulfate expression levels comparable to SCR (verified by flow cytometry, see results).
- **A549-610**: contains functional *B3GAT3*-targeting shRNA that successfully knocks down *B3GAT3* expression, resulting in significantly reduced surface heparan sulfate levels (verified by flow cytometry, see results).

These cell lines were routinely cultured in complete DMEM medium, maintained in T75 flasks, and passaged every 2 days to ensure optimal growth conditions.

Culture media and solutions

The composition of the media used for the growth of *P. aeruginosa* PAO1 and the human cell lines is reported below:

Luria-Bertani (LB) Agar, used for routine growth and plating of *P. aeruginosa* colonies.

Bacto-tryptone	10 g/L
Yeast extract	5 g/L
NaCl	10 g/L
Agar	18 g/L

The medium was sterilized in an autoclave at 118°C for 20 minutes.

Muller-Hinton II (MH-II) broth, used for checkerboard assays and determination of MIC values.

Beef extract	3 g/L
Casein acid hydrolysate	17.5 g/L
Starch	1.5 g/L

The medium was sterilized in an autoclave at 118°C for 20 minutes.

Tryptic Soy Broth (TSB), used for liquid cultures of *P. aeruginosa* PAO1 prior to adhesion assays.

Pancreatic casein digest	17 g/L
Soy peptone	3 g/L
Glucose	2.5 g/L
NaCl	5 g/L
Dipotassium hydrogen phosphate	2.5 g/L

The medium was sterilized in an autoclave at 118°C for 20 minutes.

Dulbecco's modified Eagle's medium (DMEM), a standard commercially available medium, was supplemented with 10% heat-inactivated fetal bovine serum (FBS), 0.1

mM MEM non-essential amino acids, 100 U/mL penicillin and 0.1 mg/mL streptomycin (complete DMEM) and routinely used as growth medium for the culture of human cell lines.

Phosphate buffered saline (PBS) was used as standard buffer for washing and resuspension of human cells in all described procedures. PBS composition is: 10 mM phosphate buffer, 2,7 mM potassium chloride and 137 mM sodium chloride, pH 7.4.

Normal saline (0.9% NaCl) was used for washing bacterial pellets and for preparing serial dilutions for CFU counting. The solution is obtained by dissolving NaCl at 0.9% (w/v) in distilled water and sterilizing the solution in an autoclave at 118°C for 20 minutes.

Antibiotics

The antibiotics used in this study included:

Ceftazidime, a β-lactam antibiotic used to treat severe infections caused by Gram-negative bacteria, was employed in combination with PDSTP in checkerboard assays against *P. aeruginosa* PAO1.

Rifampicin, primarily used for the treatment of tuberculosis but also active against some Gram-negative and Gram-positive bacteria, was also tested in combination with PDSTP in checkerboard assays against *P. aeruginosa* PAO1. It inhibits the initiation of RNA synthesis by binding to the β subunit of RNA polymerase, leading to bacterial cell death.

Compounds

PDSTP, a synthetic dispirotripiperazine derivative, was synthesized by our collaborator Dr. Vadim Makarov at the Research Center for Biotechnology RAS (Moscow, Russia). PDSTP was evaluated in this study as an antibiotic adjuvant and anti-adhesion compound against *P. aeruginosa* PAO1; specifically, it was tested in cytotoxicity assays on A549 cells, in checkerboard assays with ceftazidime and rifampicin, and in bacterial adhesion assays on A549-derived cell lines to investigate its effects on bacterial growth and host-pathogen interactions.

Purified lipopolysaccharide (LPS) from *P. aeruginosa* PA10 (Merck) was used as a competitor for PDSTP binding in checkerboard and adhesion assays, in order to evaluate the role of bacterial LPS as a primary target of PDSTP on the outer membrane.

Heparinase III from *Flavobacterium heparinum* (Merck) was used to enzymatically remove heparan sulfate (HS) from the surface of A549 cell monolayers before flow cytometry and adhesion assays, allowing the assessment of the contribution of host cell HS to PDSTP-mediated anti-adhesion effect.

MTT colorimetric assay for the assessment of PDSTP cytotoxicity towards human cells

A549 cells were detached from the cell culture flask using 2 mL of trypsin-EDTA and transferred to a 15 mL Falcon tube containing 8 mL of complete DMEM. The cell suspension was centrifuged at 1,200 rpm for 5 min at room temperature and the resulting pellet was resuspended in 5 mL of complete DMEM. Cells were quantified using an automated cell counter, diluted at the appropriate concentration and 200 µL of the suspension were seeded in cell culture-treated 96-well plates at a density of 4×10^4 cells per well. For each experimental condition, three technical replicates were prepared. Cells were incubated overnight (O/N) at 37°C in a humidified incubator with 5% CO_2 to allow the formation of monolayers.

After incubation, the culture medium was removed and cells were exposed for 24h to increasing concentrations of PDSTP (64, 128, 256, 512 and 1024 µg/mL) prepared by serial dilution of a stock solution in sterile PBS (100 µL per well). Cells treated with 100 µL of PBS alone were used as control. After 24h of incubation at 37°C, the supernatant was discarded and cells were washed with 100 µL of sterile PBS to remove PDSTP and any dead cells. Next, 100 µL of 3-(4,5-dimethylthiazol-2-yl)-2,5-diphenyltetrazolium bromide (MTT) solution (0.5 mg/mL in sterile PBS) were added to each well and plates were incubated for 2h at 37°C. For this assay, MTT reagent is dissolved in water, producing a yellowish solution, and, when incubated with cells, it is metabolized by mitochondrial enzymes to insoluble purple formazan crystals, allowing the quantification of metabolically active (live) cells in the sample. Indeed, once formazan is solubilized with DMSO, the colour intensity of the solution is proportional to the number of living cells. After incubation, the supernatant was carefully removed

and 100 µL per well of DMSO were added, pipetting few times to completely dissolve formazan crystals within the cells. Absorbance was measured at 560 nm using a GloMax Discover microplate reader (Promega), and cell viability was expressed as percentage relative to untreated control cells.

Checkerboard assays in the presence of PDSTP-binding competitors

Checkerboard assays were used to evaluate PDSTP antibiotic adjuvant efficacy with ceftazidime and rifampicin, against *P. aeruginosa* PAO1, in the presence or absence of an excess of Mg^{2+} or purified exogenous LPS. The day before the experiment, *P. aeruginosa* PAO1 was inoculated in 2 mL of Mueller-Hinton II (MH-II) broth and grown O/N at 37°C with shaking (200 rpm), starting from isolated colonies grown on a LB agar plate. On the following day, 100 µL of the O/N culture were inoculated into 10 mL of fresh MH-II broth (1:100 dilution) and incubated at 37°C with shaking until reaching the mid-log phase, corresponding to an optical density at 600 nm (OD_{600}) of approximately 0.5. This culture served as the inoculum for the checkerboard assay.

The experiment was prepared in sterile 96-well microtiter plates with two-fold serial dilutions of PDSTP and antibiotics along the two axes of the plate. For plate layout, a concentration gradient of PDSTP ranging from 1 to 64 µg/mL was established along rows A-G, while a gradient of ceftazidime (0.003-2 µg/mL) or rifampicin (0.062-32 µg/mL) was established along columns 3-12. Row H and column 2 were used to determine the minimum inhibitory concentrations (MICs) of the individual compounds.

To prepare the PDSTP gradient, a stock solution was diluted in MH-II broth to obtain a concentration four-fold higher than the desired final concentration in row A (64 µg/mL). 95 µL of MH-II were dispensed into all wells, and 95 µL of the PDSTP working solution were added to each well of row A, except column 1. Two-fold serial dilutions were performed by transferring 95 µL from row A down to row G, and the final 95 µL taken from row G were discarded, so that row H did not contain PDSTP.

For the antibiotic gradients, working solutions of ceftazidime and rifampicin were prepared in MH-II at concentrations 40-fold higher than the desired final concentrations. From these, series of two-fold dilutions were prepared in Eppendorf tubes to generate the ranges 0.003-2 µg/mL (ceftazidime) and 0.062-32 µg/mL (rifampicin), corresponding to columns 3-12. Then, 5 µL of each antibiotic dilution were added to the wells of the appropriate column, resulting in a total volume of 100 µL per well before bacterial inoculation.

Once the plate was prepared, mid-log phase (OD_{600}=0.5) bacterial culture was diluted in MH-II broth to obtain a concentration of approximately 1×10^5 CFU/mL. 100 µL of this diluted culture were added to each well, except for those in column 1, which served as negative controls and contained medium only. Additional wells containing bacteria but no compounds were included as growth controls. When specified, 20 mM $MgCl_2$ or 200 µg/mL *P. aeruginosa* PA10 purified LPS (Merck) were included in the bacterial inoculum, ensuring that these concentrations were present throughout the checkerboard matrix. Parallel control experiments without $MgCl_2$ or purified LPS were prepared. Once plates were ready, they were then incubated O/N at 37°C.

The following day, bacterial growth was assessed using resazurin. Resazurin is a non-fluorescent dye that is reduced to a highly fluorescent molecule, called resorufin, by the bacterial metabolism. This reaction allows us to detect bacterial growth by measuring the fluorescence of each well. Thirty microliters of a 0.01% (w/v) resazurin solution were added to each well, and plates were further incubated at 37°C for 3h. Fluorescence of the resulting resorufin was measured using a GloMax Discover microplate reader (Promega) with an excitation wavelength of 520 nm and an emission range of 580-640 nm.

The interaction between PDSTP and each antibiotic was evaluated by calculating the fractional inhibitory concentration (FIC) index, defined as the sum of FIC_A and FIC_B:

$$FIC_A = \frac{MIC_{(A\ in\ the\ presence\ of\ B)}}{MIC_A} \qquad FIC_B = \frac{MIC_{(B\ in\ the\ presence\ of\ A)}}{MIC_B}$$

FIC values < 0.5 were interpreted as synergistic, between 0.5-1.0 as additive, between 1.0-2.0 as indifferent, and > 2.0 as antagonistic.

Adhesion assays of *P. aeruginosa* PAO1 on A549 cell monolayers

Epithelial cells were detached, resuspended, and diluted in antibiotic free DMEM (see MTT assay paragraph for details) to obtain a final concentration of 1.5×10^5 cells/mL. Cells were then seeded in cell culture-treated 24-well plates at 1 mL per well and incubated O/N at 37°C in a humidified incubator with 5% CO_2. The following day, the medium was replaced with fresh antibiotic free DMEM and plates were incubated for another 24h at 37°C. In parallel, *P. aeruginosa* PAO1 was grown O/N in TSB broth at 37°C with shaking. The next day, the bacterial culture was diluted 1:100 in 10 mL of TSB and incubated at 37°C with shaking until reached an OD_{600}=0.5. An aliquot of 5

mL of the bacterial suspension was collected and centrifuged at 5000 rpm for 8 min at 10°C. The supernatant was discarded and the bacterial pellet was washed once with 5 mL of normal saline, centrifuged again, and finally resuspended in 5 mL of antibiotic free DMEM. Bacterial suspensions were prepared in the same medium at a final concentration of 2.5×10^6 CFU/mL, corresponding to a multiplicity of infection of 10 bacteria per cell (MOI 10).

To start the adhesion assay, the culture medium was removed from the A549 monolayers and replaced with 1 mL of the MOI 10 bacterial suspension per well. PDSTP (25, 50 or 200 µg/mL) and/or binding competitors (20 mM $MgCl_2$ or 200 µg/mL purified LPS), when appropriate, were added directly into the corresponding wells. Untreated wells and wells treated with a single compound were used as bacterial adhesion controls. Plates were incubated for 2h at 4°C to allow bacterial adhesion.

After incubation, non-adherent bacteria were removed by washing the monolayers three times with sterile PBS. Cells were then lysed with 500 µL of 0.1% Triton X-100 in PBS to release cell-associated bacteria. Lysates were serially diluted in normal saline, and 100 µL of the appropriate dilutions were plated in duplicate on LB agar plates. Plates were incubated O/N at 37°C. The following day, colonies were counted to determine the number of adherent bacteria in the different conditions, expressed as CFU per well.

Adhesion assays of *P. aeruginosa* PAO1 on A549 monolayers after Heparinase III treatment

A549 cells were detached, resuspended, and diluted in antibiotic free DMEM to obtain a final concentration of 1.5×10^5 cells/mL. Cells were seeded in 24-well plates at 1 mL per well and incubated O/N at 37°C in a humidified incubator with 5% CO_2. On the following day, the medium was replaced with fresh DMEM and cells were incubated for an additional 24h at 37°C, 5% CO_2.

On the day of the experiment, medium was removed and monolayers were washed once with sterile PBS. To remove HS, cells were enzymatically treated with 100 mU of Heparinase III (Merck) in PBS supplemented with 0.01% BSA, 1.5 mM $CaCl_2$ at 37°C for 2h. After incubation, Heparinase III solution was discarded and monolayers were washed twice with PBS prior to infection. The further steps of the protocol, including monolayer infection and treatment, incubation and quantification of the adherent bacteria were carried out as already described in the "Adhesion assays of *P. aeruginosa* PAO1 on A549 cell monolayers" paragraph.

Immunofluorescence analysis of heparan sulfate expression on A549 cell surface

Glass coverslips were cleaned with 70% ethanol and briefly passed over a flame for sterilization. Thereafter, they were placed in 60 mm Petri dishes and seeded with 3×10^5 A549 cells in 900 µL of complete DMEM. Cells were incubated for 2h at 37°C, 5% CO_2, to allow the adhesion to the coverslips, after which 3 mL of complete DMEM were added.

Following O/N incubation at 37°C, 5% CO_2, the medium was removed and monolayers were washed three times for 5 minutes with 4 mL of PBS. Cells were fixed with 3 mL of 4% paraformaldehyde for 30 minutes on ice and then washed three times with PBS. Non-specific binding sites for antibodies were blocked by incubating monolayers for 1h at room temperature in 4 mL of PBS containing 1% Tween 20 and 1% skimmed milk, followed by three washes with PBS.

Cell monolayers were then incubated for 1h at room temperature with a solution of PBS, 1% Tween 20, 1% skimmed milk containing the primary anti-heparan sulfate F58-10E4 mouse antibody diluted 1:100. To remove unbound antibodies, they were washed three times with PBS and then incubated for 1h at room temperature, in the dark, with secondary antibody diluted 1:200 in the same buffer. Lastly, cells were washed three additional times with PBS. Coverslips were mounted, cell-side down, onto glass microscope slides using ProLong Gold Antifade Mountant containing DAPI dye for nuclear staining. Slides were stored at 4°C in the dark until image acquisition using a Leica DM6 B widefield fluorescence microscope. To check the specificity of the fluorescence signal, control samples stained only with the secondary antibody were included.

Flow cytometry immunofluorescence analysis of heparan sulfate expression on A549-SCR and *B3GAT3*-KDs cell surfaces

A549-SCR, 609 and 610 cell lines were seeded at 3×10^5 cells per well in antibiotic free DMEM into cell culture-treated 24-well plates and incubated O/N at 37°C, 5% CO_2. The following day, medium was replaced with fresh antibiotic free DMEM and plates were incubated for another 24h at 37°C, 5% CO_2.

On the day of the experiment, cells were gently detached using Accutase solution (Merk), to preserve most surface cell markers, transferred to 1.5 mL Eppendorf tubes, and centrifuged at 1200 rpm for 5 minutes at room temperature. Pellets were washed with 2 mL of PBS and resuspended in 1 mL of PBS + 10% FBS for blocking

non-specific antibodies binding sites. Then, cells were counted, and aliquots of 2×10^5 cells were prepared and washed at 4°C with 1 mL of PBS. Pellets were resuspended in 100 µL PBS + 3% bovine serum albumin (BSA) containing the primary anti-heparan sulfate F58-10E4 mouse antibody (diluted 1:100), and incubated for 40 minutes at 4°C. After that, samples were washed twice with PBS at 4°C, resuspended in 100 µL PBS + 3% BSA containing the secondary rhodamine (TRITC) goat anti-mouse IgM antibody (diluted 1:200), and incubated for 40 minutes at 4°C in the dark. After two PBS washes at 4°C, cells were resuspended in 200 µL of PBS + 10% FBS, kept on ice protected from light and immediately analysed by BD FACSLyric flow cytometry system; for the analysis, at least 22.000 events were collected for each sample. To check the specificity of the fluorescence signal, control samples stained only with the secondary antibody were included.

Flow cytometry immunofluorescence analysis of heparan sulfate on A549 cell surface after Heparinase III treatment

A549 cells were seeded at 3×10^5 cells per well in antibiotic free DMEM into cell culture-treated 24-well plates and incubated O/N at 37°C, 5% CO_2. The following day, medium was replaced with fresh antibiotic free DMEM and plates were incubated for another 24h at 37°C, 5% CO_2. To cleave HS from cell surface, growth medium was removed and monolayers were washed twice with PBS before incubating them at 37°C for 2h with 100 mU of Heparinase III in PBS supplemented with 0.01% BSA, 1.5 mM $CaCl_2$. After 2 h, reactions were stopped by removing the enzyme and washing wells three times with 1 mL of PBS. Samples for flow cytometry analysis were prepared following the protocol already described in the "Flow cytometry immunofluorescence analysis of heparan sulfate expression on A549-SCR and *B3GAT3*-KDs cell surfaces" paragraph.

RESULTS AND DISCUSSION

Assessment of PDSTP cytotoxicity towards human cells

The cytotoxic profile of PDSTP was initially characterized on human A549 lung epithelial cells through the MTT colorimetric assay, which assesses mitochondrial metabolic activity as an indicator of cell viability. A549 cells were exposed to increasing PDSTP concentrations (64, 128, 256, 512, and 1024 µg/mL) for 24 hours during safety screening for antimicrobial compound testing.

Results, expressed as percentage viability relative to untreated control cells (set at 100%), are presented in **Figure 22** (n=3 independent experiments, performed in triplicate).

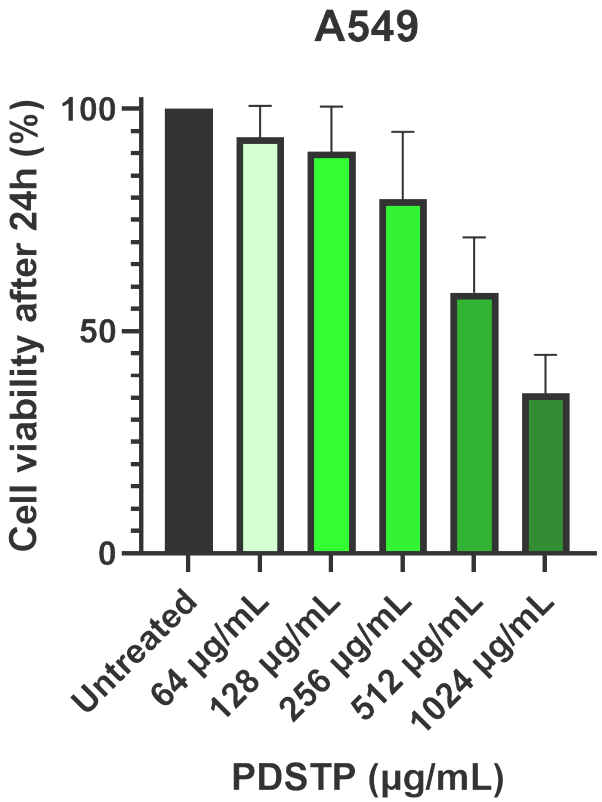

***Figure 22**. Effect of PDSTP on A549 cell viability after 24h of treatment. A549 cells were exposed to increasing concentrations of PDSTP (64-1024 µg/mL) for 24h, and cell viability was assessed by MTT assay and expressed as percentage of the untreated control (mean ± SD of three technical replicates).*

At the lowest concentrations tested (64 and 128 µg/mL), PDSTP did not substantially affect A549 cell viability, with values remaining consistently above 95% of control levels.

A modest reduction in viability (~80-85%) was observed at 256 µg/mL, suggesting only minimal metabolic stress. This concentration marks the upper limit selected for following functional assays (checkerboard and adhesion).

In contrast, higher concentrations induced a clear dose-dependent cytotoxic response. At 512 µg/mL, cell viability dropped to approximately 50-60% of control values. The effect intensified further at 1024 µg/mL, yielding the lowest viability readings observed.

Overall, these data demonstrate that PDSTP is relatively non-toxic to A549 cells at concentrations up to 256 µg/mL after 24h of treatment, whereas cytotoxic effects become progressively more evident at 512 and 1024 µg/mL. Although these higher concentrations are useful to define the upper cytotoxic range *in vitro*, they exceed acceptable therapeutic doses. Therefore, only concentrations ≤256 µg/mL were used in following experiments.

Adjuvant activity of PDSTP with ceftazidime in the presence of $MgCl_2$ or LPS

The checkerboard assays were performed to measure the adjuvant properties of PDSTP with ceftazidime against *P. aeruginosa* PAO1, while assessing the influence of $MgCl_2$ (20 mM) or exogenous LPS (200 µg/mL PA10 LPS). The following heatmaps represent metabolic activity (dark green=full growth/viability; light green=decreased growth; white=growth inhibition; n=3, biological replicates).

In the absence of additives, increasing concentrations of PDSTP shifted the inhibitory effect of ceftazidime towards lower concentrations, as indicated by the expansion of the low-signal area at intermediate PDSTP doses (**Fig. 23**). This pattern was consistent with an additive to mildly synergistic interaction between PDSTP and ceftazidime under standard conditions.

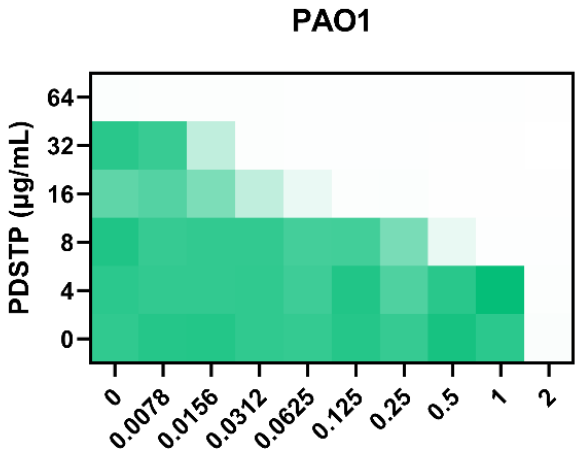

***Figure 23**: Checkerboard heatmap of PDSTP-ceftazidime interaction against P. aeruginosa PAO1 under standard conditions (dark green=full growth/viability; light green=decreased growth; white=growth inhibition; n=3, biological replicates).*

When 20 mM $MgCl_2$ was added to the medium (**Fig. 24**), this synergistic effect was lost. Unlike standard conditions, high metabolic activity persisted across nearly all PDSTP/ceftazidime combinations, even at intermediate PDSTP doses (16-32 µg/mL) where synergy was evident without $MgCl_2$. The low-signal inhibitory region was greatly reduced, with bacterial viability remaining >80% in most wells. Mg^{2+} ions, known to stabilize LPS-outer membrane interactions, likely competitively inhibit PDSTP binding to bacterial LPS.

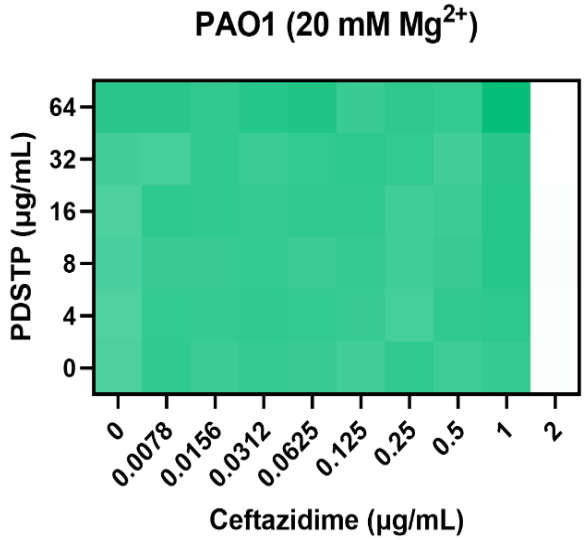

***Figure 24**: Effect of 20 mM $MgCl_2$ on PDSTP-ceftazidime interaction against PAO1 (dark green=full growth/viability; light green=decreased growth; white=growth inhibition; n=3, biological replicates).*

Similarly, the presence of 200 µg/mL exogenous *P. aeruginosa* LPS also diminished the PDSTP's adjuvant activity (**Fig. 25**). High metabolic activity was observed across most PDSTP/ceftazidime combinations, with the low-signal inhibitory region markedly reduced compared to standard conditions (i.e. in the absence of purified LPS). These findings suggest that an excess of soluble LPS acts as a competitive inhibitor, preventing PDSTP interaction with bacterial surface LPS.

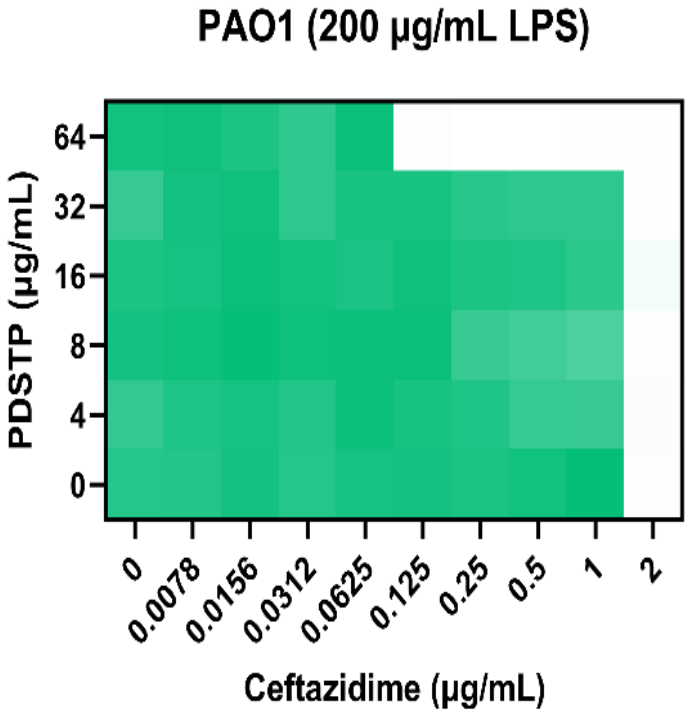

***Figure 25**: Effect of 200 µg/mL exogenous P. aeruginosa PA10 LPS on PDSTP-ceftazidime interaction (dark green=full growth/viability; light green=decreased growth; white=growth inhibition; n=3, biological replicates).*

Together, these data indicate that PDSTP potentiates ceftazidime activity against PAO1 through LPS-dependent mechanisms, as both Mg^{2+} and an excess of soluble LPS counteracted the adjuvant effect, supporting the hypothesis of PDSTP-LPS interactions at the bacterial surface.

Adjuvant activity of PDSTP with rifampicin in the presence of $MgCl_2$ or LPS

A parallel checkerboard approach was used to assess PDSTP adjuvant properties with rifampicin, a hydrophobic antibiotic with completely different mechanism of action from ceftazidime, against *P. aeruginosa* PAO1 under identical conditions (20 mM $MgCl_2$; 200 µg/mL PA10 LPS). Heatmaps show metabolic activity (dark blue=full

growth/viability; light blue=decreased growth; white=growth inhibition; n=3, biological replicates).

In the absence of additives, increasing concentrations of PDSTP shifted the inhibitory effect of rifampicin towards lower antibiotic concentrations, as indicated by the expansion of the low-signal area at intermediate PDSTP doses (**Fig. 26**).
This pattern was consistent with an additive to mildly synergistic interaction between PDSTP and rifampicin under standard conditions.

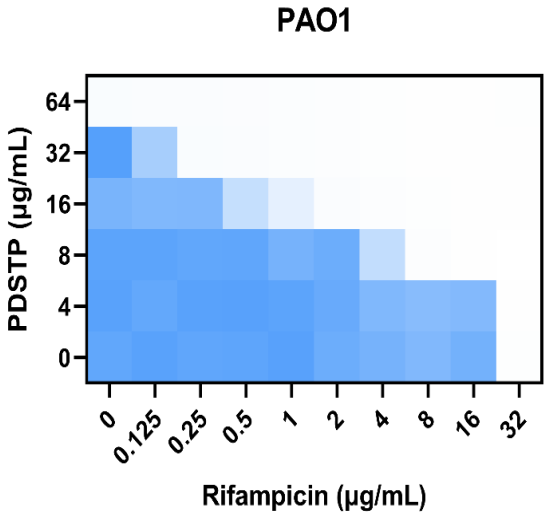

***Figure 26**: Checkerboard heatmap PDSTP-rifampicin vs PAO1 (standard) (dark blue=full growth/viability; light blue=decreased growth; white=growth inhibition; n=3, biological replicates).*

When 20 mM $MgCl_2$ was added to the medium (**Fig. 27**), this synergistic effect was lost. Unlike standard conditions, high metabolic activity persisted across nearly all PDSTP/rifampicin combinations, even at intermediate PDSTP doses (16-32 µg/mL) where synergy was evident without $MgCl_2$. The low-signal inhibitory region was greatly reduced, with bacterial viability remaining >80% in most wells. As already reported for ceftazidime, Mg^{2+} ions interfered with PDSTP adjuvant effect, competitively inhibiting PDSTP binding to bacterial LPS.

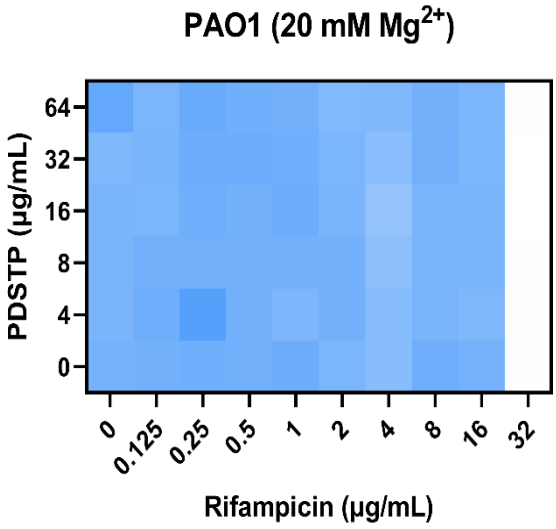

***Figure 27**: Effect of 20 mM Mg^{2+} on PDSTP-rifampicin interaction against PAO1 (dark blue=full growth/viability; light blue=decreased growth; white=growth inhibition; n=3, biological replicates).*

Similarly, the presence of 200 µg/mL exogenous *P. aeruginosa* LPS also diminished PDSTP's adjuvant activity (**Fig. 28**). High metabolic activity was observed across most PDSTP/rifampicin combinations, with the low-signal inhibitory region markedly reduced compared to standard conditions. These findings further confirm that an excess of soluble LPS acts as a competitive inhibitor, preventing PDSTP interaction with bacterial surface LPS. Moreover, these results proved that ceftazidime and rifampicin potentiation is mediated by the same mechanism.

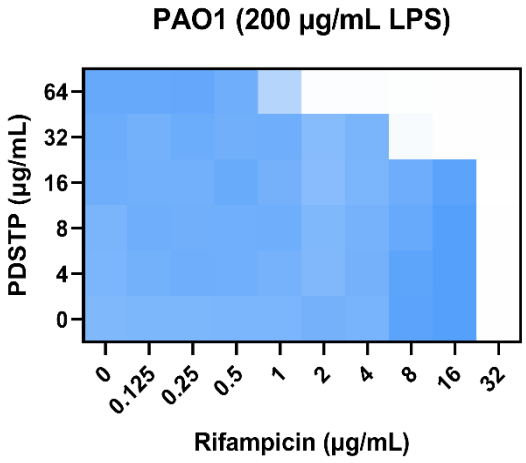

***Figure 28**: Effect of 200 µg/mL exogenous P. aeruginosa PAO1 LPS on PDSTP-rifampicin interaction (dark blue=full growth/viability; light blue=decreased growth; white=growth inhibition; n=3, biological replicates).*

Effect of $MgCl_2$ and of purified LPS on the adhesion of *P. aeruginosa* PAO1 to A549 cell monolayers

The ability of PDSTP to inhibit *P. aeruginosa* PAO1 adhesion to A549 cells was evaluated in the absence or presence of $MgCl_2$ and exogenous LPS to further assess if its mechanism of action involves an interaction with surface LPS. Bacterial adhesion was quantified after 2h of incubation at 4°C, as previously described (Bonacorsi *et al.*, 2024), and expressed as percentage relative to the untreated control (set as 100%).

In the absence of competitors, treatment with PDSTP at 50 µg/mL greatly reduced PAO1 adhesion to A549 monolayers, significantly decreasing the number of adherent bacteria to roughly one-third respect to control levels (**Fig. 29**). This result confirms the strong anti-adhesion activity of PDSTP observed in previous experiments (Bonacorsi *et al.*, 2024).

The addition of 20 mM $MgCl_2$ alone did not significantly modify bacterial adhesion compared with the untreated control, indicating that this concentration of Mg^{2+} does not directly affect PAO1 binding to A549 cells. However, when $MgCl_2$ was combined with 50 µg/mL PDSTP, the anti-adhesion effect of the compound was completely impaired, and adhesion levels returned close to those of the control condition (**Fig. 29**).

These data suggest that an excess of Mg^{2+} interferes with PDSTP-mediated inhibition of adhesion, most likely by shielding negatively charged groups on bacterial LPS and/or on the host cell surface that are required for PDSTP to exert its effect.

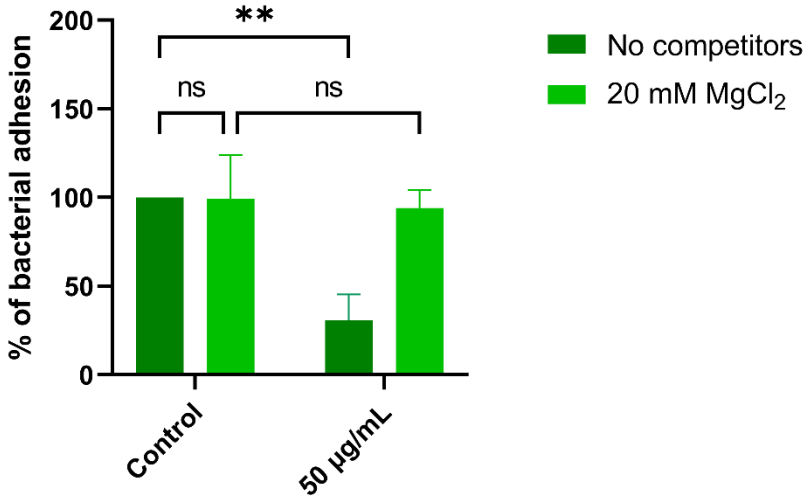

***Figure 29**: Adhesion of P. aeruginosa PAO1 to A549 monolayers in the presence of PDSTP (50 µg/mL) and $MgCl_2$ (20 mM, light green bar). Statistical test: two-way ANOVA, **: p<0.005, ns: not significant.*

A complementary set of experiments was performed to assess the impact of exogenous LPS on PDSTP activity. The addition of 200 µg/mL of purified *P. aeruginosa* LPS alone slightly increased PAO1 adhesion to A549 cells, but this effect did not reach statistical significance respect to the untreated control (**Fig. 30**).

In contrast, when LPS was co-incubated with PDSTP at 25 µg/mL, the marked reduction in bacterial adhesion observed with PDSTP alone was completely lost, and adhesion levels were comparable to those of the control. This indicates that soluble LPS efficiently competes with bacterial surface LPS for PDSTP binding, thereby preventing the compound from exerting its anti-adhesion effect at the host-pathogen interface.

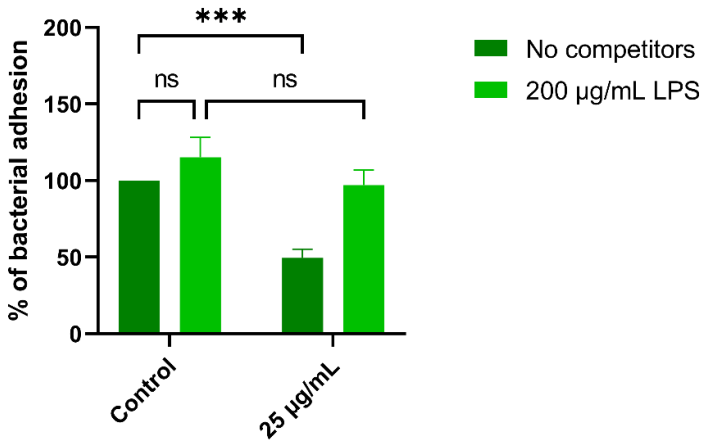

***Figure 30**: Adhesion of P. aeruginosa PAO1 to A549 monolayers in the presence of PDSTP (25 µg/mL) and exogenous PA10 LPS (200 µg/mL, light green bar). Statistical test: two-way ANOVA, ***: p<0.001, ns: not significant.*

Taken together, these results show that PDSTP significantly reduces PAO1 adhesion to A549 cells, but its anti-adhesion activity is strongly impaired by high concentrations of Mg^{2+} and by the addition of exogenous purified LPS. This supports the hypothesis that PDSTP acts primarily through electrostatic interactions with bacterial LPS, and that modulation of LPS availability or charge can critically influence its ability to block bacterial adhesion.

Immunofluorescence analysis of heparan sulfate expression on A549 cell surface

To assess the putative role of heparan sulfate (HS) proteoglycans as mediators of PDSTP anti-adhesion effect, their expression on human A549 lung epithelial cells was analysed by immunofluorescence using the F58-10E4 monoclonal antibody (Amsbio), which specifically recognises native HS chains on the cell surface.

Cells were fixed, minimally permeabilised to preserve surface localisation, and nuclei were counterstained with DAPI to visualise morphology and confluence.

The acquired images (**Fig. 31**) revealed an intense, widespread HS-associated red fluorescence outlining the plasma membrane of A549 cells, with characteristic finely punctate distribution along cell protrusions. This pattern confirms abundant HS localisation at the cell-medium interface, consistent with its role as co-receptor for bacterial adhesins. Even though a small amount of intracellular staining was observed, this labelling was confirmed as mainly surface-specific, supporting A549 cells as suitable model for investigating HS-dependent *P. aeruginosa* adhesion and PDSTP interactions in following experiments.

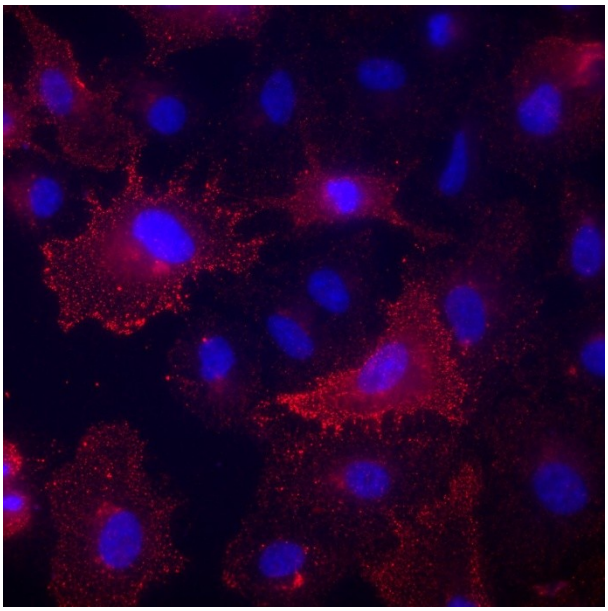

***Figure 31**: Indirect immunofluorescence of HS (10E4, red) on A549 cells. Nuclei were stained with DAPI and are visible in blue).*

Evaluation of heparan sulfate expression on A549-SCR, A549-609 and A549-610 cell surfaces by flow cytometry immunofluorescence

Surface HS expression was quantified by flow cytometry on three A549-derived cell lines engineered for differential *B3GAT3*/HS expression:

- **A549-SCR** (scrambled control): transduced with non-targeting shRNA (random sequence), maintains normal HS surface expression as negative control;
- **A549-609**: contains ineffective *B3GAT3*-targeting shRNA (no gene knockdown achieved), HS levels comparable to SCR;
- **A549-610**: features functional *B3GAT3*-targeting shRNA with successful gene knockdown, resulting in significantly reduced surface HS expression.

Cells were detached with Accutase, blocked (PBS+10% FBS), stained with anti-HS F58-10E4 monoclonal antibody (1:100) followed by TRITC-conjugated goat anti-mouse IgM secondary antibody (1:200) at 4°C. Flow cytometry analysis was performed on BD FACSLyric (≥22,000 events/sample; n=3 biological replicates; **Fig. 32**).

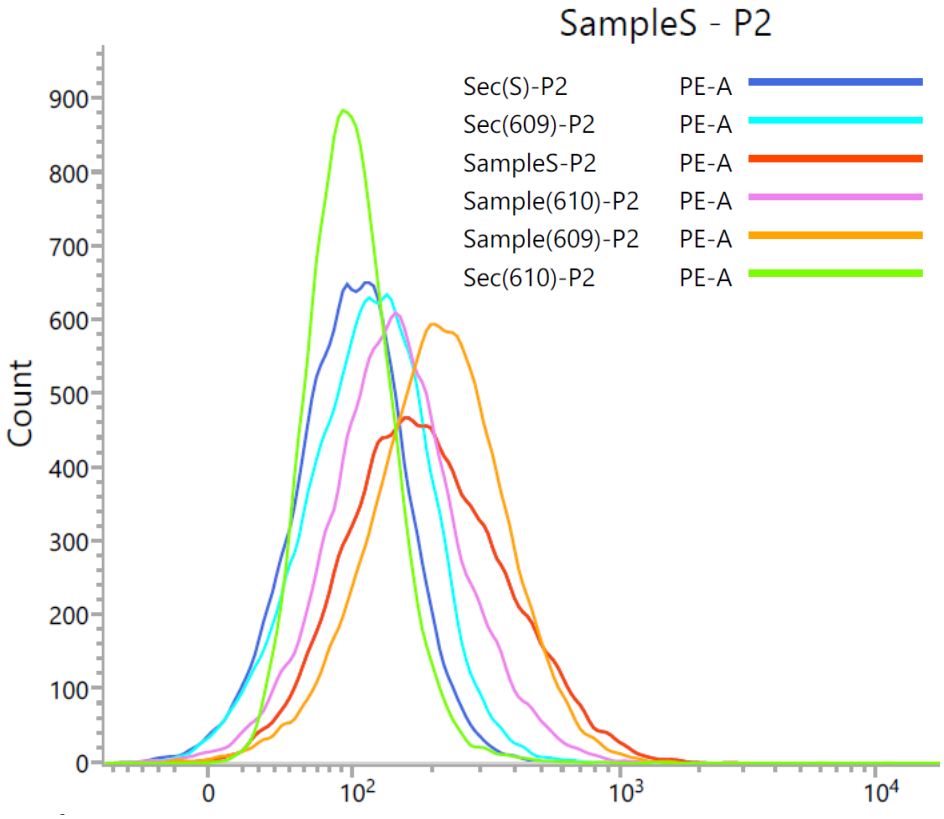

***Figure 32**: Flow cytometry graph of HS expression on A549-derived cell lines. A549-SCR (SampleS, red), A549-609 (Sample(609),orange), A549-610 (Sample(610), pink) stained with anti-HS 10E4 primary antibody +TRITC secondary antibody, versus secondary antibody-only controls Sec(S/609/610).*

SCR (SampleS, red) and 609 (Sample(609), orange) displayed overlapping high HS fluorescence profiles (rightward peak position), confirming 609 shRNA inefficiency and establishing SCR as reliable high-HS baseline. Critically, 610 *B3GAT3* KD (Sample (610), pink) showed a pronounced leftward shift demonstrating successful surface HS knockdown. The overlay clearly separates 610 (pink, low HS) from SCR/609 peaks (red/orange, high HS), with secondary antibody controls Sec(S) (no primary Ab) confirming signal specificity. These data validate A549-610 as a low-HS expressing model suitable for adhesion assays probing PDSTP host dependency, while SCR serve as high-HS expressing control.

Adhesion assays of *P. aeruginosa* PAO1 on A549-SCR and A549-610 (*B3GAT3* knockdown) cell monolayers

As described in the Introduction, for its antiviral activity PDSTP primarily targets HS on respiratory epithelial cells, where its quaternary positively charged nitrogen atoms engage electrostatic interactions with the sulfate groups of HS, effectively blocking adhesion. Since also many bacteria, including *P. aeruginosa*, use HS as receptors for host-pathogen interactions (García *et al*., 2016), the impact of HS removal on PDSTP anti-adhesion effect was evaluated by using A549 cells genetically modified knocking down the *B3GAT3* gene (A549-610, low HS expression) and compared to lentiviral scramble control (A549-SCR high HS expression). Bacterial adhesion was quantified after 2h incubation at 4°C and expressed as percentage relative to untreated control.

PAO1 adhesion to A549-610 (*B3GAT3*KD) monolayers was not significantly different from A549-SCR (scrLV) cells (**Fig. 33**), demonstrating that reduced HS levels do not impair *P. aeruginosa* binding to host cells.

PDSTP treatment at 50 µg/mL and 200 µg/mL strongly inhibited the adhesion of *P. aeruginosa* to both cell lines, reducing adherent bacteria to 35-40% and 15-20% respect to control levels, with no significant difference between SCR and 610 conditions (**Fig. 33**).

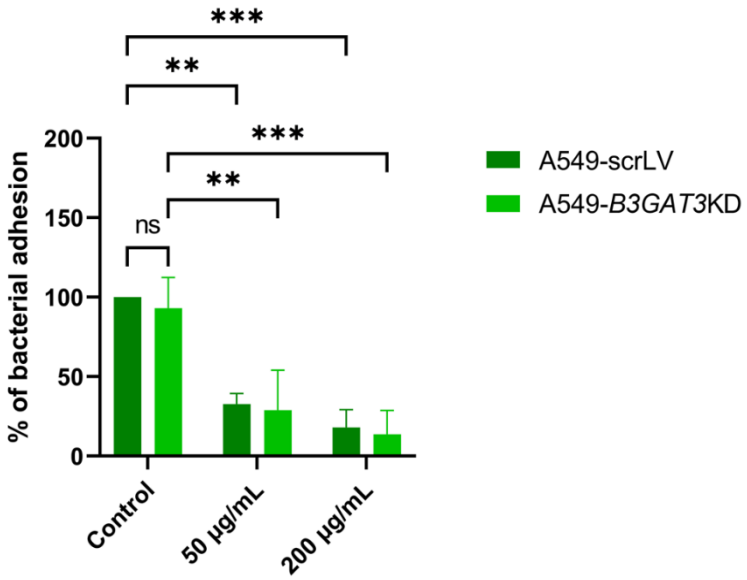

***Figure 33**: Adhesion of P. aeruginosa PAO1 to A549-scramble lentiviral (SCR, dark green bar) and A549-B3GAT3 knockdown (610, light green bar) monolayers in the presence of PDSTP (50, 200 µg/mL). Statistical test: two-way ANOVA, **: p<0.005, ***: p<0.001, ns: not significant.*

These findings demonstrate that low HS expression neither impairs PAO1 adhesion nor diminishes PDSTP efficacy, strongly supporting bacterial surface LPS, rather than host HSPGs, as the primary molecular target mediating PDSTP anti-adhesion activity.

Evaluation of heparan sulfate presence on A549 cell surface after Heparinase III treatment by flow cytometry immunofluorescence

To validate the results obtained using the genetically modified A549-SCR and A549-610 cell lines, enzymatic removal of HS from A549 cell surface was carried out using *F. heparinum* Heparinase III and verified by flow cytometry. A549 cells were cultured for 48h in antibiotic-free DMEM and then exposed for 2h at 37°C to Heparinase III (100 mU/mL in PBS containing 0.01% BSA and 1.5 mM $CaCl_2$) to remove surface HS. After extensive washing, cells were harvested and stained with the anti-HS 10E4 antibody followed by TRITC goat anti-mouse IgM secondary antibody, and fluorescence was recorded by flow cytometry, as described for the analysis of HS expression on A549-SCR, -609 and -610 cell lines.

Untreated A549 cells showed a fluorescence peak clearly confirming robust basal HS expression at the plasma membrane (**Fig. 34**). In contrast, Heparinase III-treated cells displayed a marked leftward shift of the peak towards substantially lower fluorescence values (**Fig. 35**), consistent with efficient cleavage of HS chains from the cell surface.

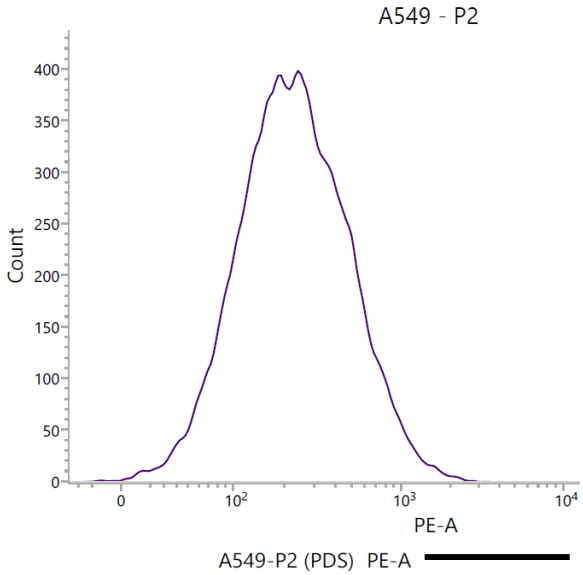

Figure 34. *Flow cytometry graph of HS expression on control A549 cells without Heparinase III treatment.*

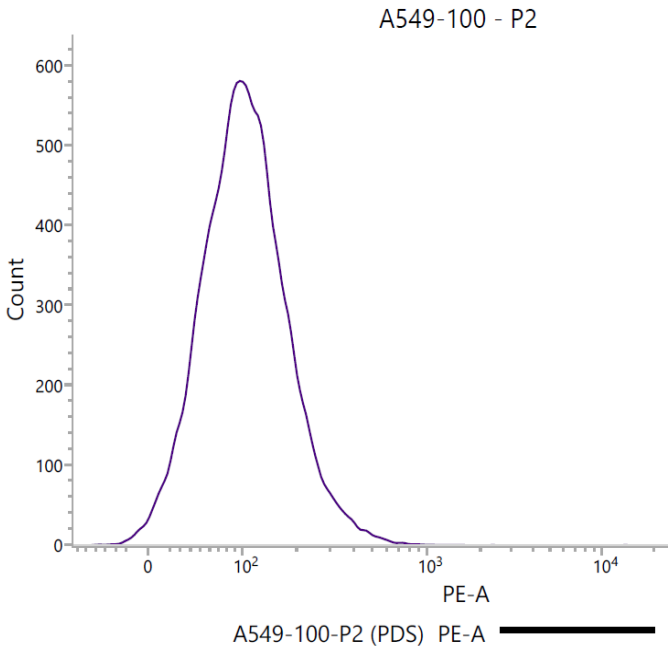

Figure 35. *Flow cytometry graph of HS expression on A549 cells treated with 100 mU/mL Heparinase III.*

The dose-dependent effect of Heparinase III **(Fig. 36)** demonstrates the enzyme's efficiency (0, 50, 100, 200 mU/mL) in removing surface HS from A549 cells. Untreated cells A549-P2 (0 mU/mL) show high fluorescence (rightward peak), while increasing enzyme concentrations induce progressive leftward shifts, approaching the secondary antibody-only control (Sec(A549)-P2) at 200 mU/mL. This confirms near-complete HS cleavage at 100-200 mU/mL, validating the enzymatic model for adhesion assays comparable to A549-610 cells.

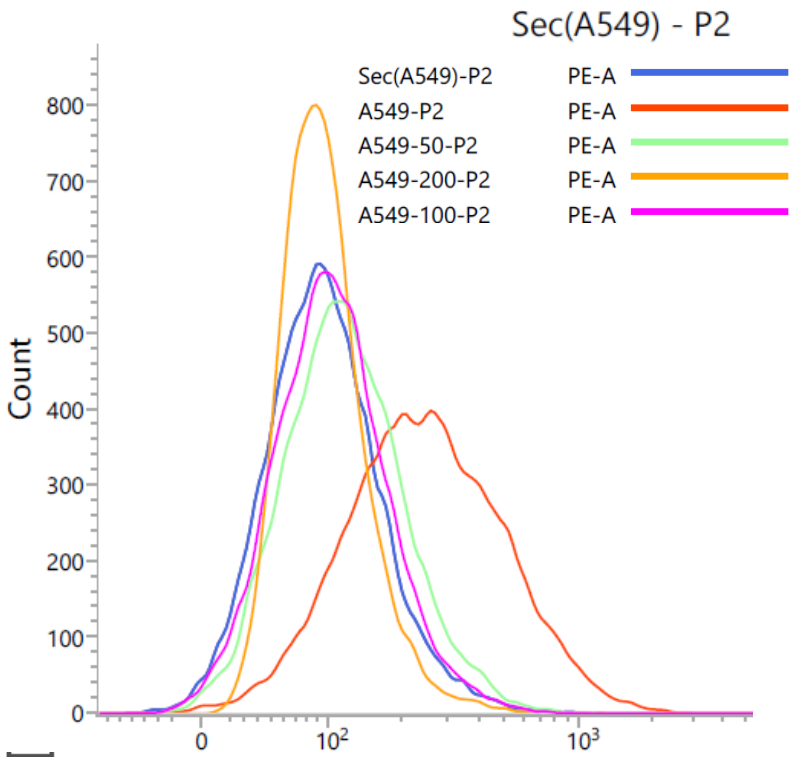

***Figure 36**. Flow cytometry of HS expression on A549 cells after Heparinase III treatment at 0, 50, 100 and 200 mU/mL compared with secondary-only control.*

Taken together, these data (**Fig. 34-36**) indicate that Heparinase III treatment induces a dose-dependent and near-complete loss of detectable HS on A549 cells, providing an HS-depleted model that can be directly compared with the genetically engineered *B3GAT3* knock-down lines in subsequent adhesion assays.

Adhesion assays of *P. aeruginosa* PAO1 on Heparinase III-treated A549 cell monolayers

The impact of HS removal on PDSTP anti-adhesion effect was evaluated by pre-treating A549 monolayers with Heparinase III prior to bacterial infection. Adherent bacteria were quantified after 2h incubation at 4°C and expressed as percentage relative to untreated control (set at 100%; n=3 biological replicates; **Fig. 37**).

Heparinase III treatment did not significantly alter PAO1 adhesion levels to A549 monolayers compared to untreated monolayers (**Fig. 37**), confirming that surface HS are not required for PAO1 binding to A549 cells.

As previously shown, PDSTP strongly inhibited the adhesion of *P. aeruginosa* to untreated monolayers, reducing adherent bacteria to approximately 30% (50 µg/mL) and 20% (200 µg/mL) respect to the control values. This anti-adhesion effect

was fully retained in Heparinase III-treated monolayers, with comparable inhibition levels (~35% and ~25% respectively; **Fig. 37**).

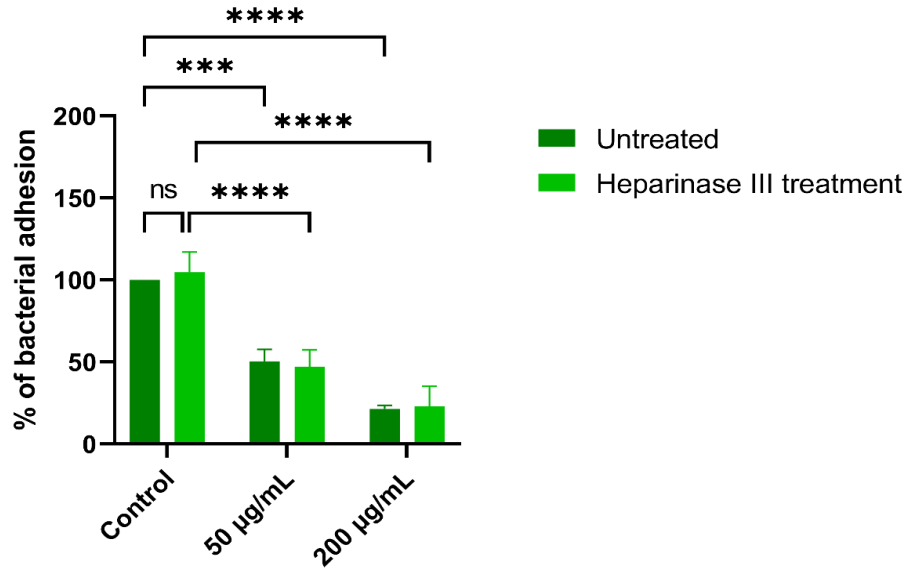

***Figure 37**: Adhesion of P. aeruginosa PAO1 to A549 monolayers ± Heparinase III treatment (light green bars) in the presence of PDSTP (50, 200 µg/mL). Statistical test: two-way ANOVA, ***: p<0.001, ****: p<0.0005, ns: not significant.*

These results mirror those obtained with A549 *B3GAT3* knockdown cells (**Fig. 33**), confirming that PDSTP anti-adhesion efficacy is fully retained in HS-depleted host cells. Altogether, genetic and enzymatic HS depletion experiments establish that host HS is neither required for PAO1 adhesion nor acts as a critical target for PDSTP, further supporting bacterial surface LPS as the primary mediator of PDSTP's anti-adhesion mechanism at the host-pathogen interface.

CONCLUSIONS

The experiments conducted in this Master's thesis have demonstrated the safety profile and therapeutic potential of PDSTP, a synthetic dispirotripiperazine derivative, as a dual-function compound exhibiting both antibiotic adjuvant activity and potent anti-adhesion effects against *Pseudomonas aeruginosa* PAO1, a major opportunistic pathogen responsible for chronic lung infections in cystic fibrosis patients.

Safety profiling on human A549 lung epithelial cells through MTT colorimetric assays established PDSTP's favourable cytotoxic profile, maintaining >95% cell viability at 64-128 µg/mL and 80-85% at 256 µg/mL. PDSTP was thus non-toxic at concentrations effective for investigating its antimicrobial adjuvant and anti-adhesion activities (1-64 µg/mL), justifying its use in all subsequent *in vitro* assays.

Antibiotic adjuvant activity was characterized through checkerboard assays combining PDSTP (1-64 µg/mL) with ceftazidime (0.003-2 µg/mL) and rifampicin (0.062-32 µg/mL) against PAO1. Under standard conditions, both combinations yielded fractional inhibitory concentration indices <0.5, suggesting synergistic interactions. PDSTP shifted antibiotic inhibitory concentrations towards lower values, expanding low-signal (inhibition) regions across heatmaps. This pattern was disrupted by the addition of 20 mM $MgCl_2$, which restored >80% bacterial viability across nearly all wells by stabilizing LPS-outer membrane bonds. Similarly, 200 µg/mL of purified exogenous PA10 LPS diminished PDSTP's adjuvant effect, with high metabolic activity persisting across most combinations. These results suggest that PDSTP's adjuvant mechanism may depend on electrostatic binding to bacterial surface LPS phosphates, potentially compromising outer membrane integrity to facilitate antibiotic penetration.

Anti-adhesion efficacy mirrored these findings. PDSTP reduced PAO1 adhesion to A549 monolayers by 70% at 50 µg/mL and >80% at 200 µg/mL, reducing adherent CFU to up to one-fifth of untreated controls. This potent inhibition was altered by the addition of $MgCl_2$ 20 mM or soluble LPS 200 µg/mL (adhesion restored to 90-100% control levels), consistent with LPS playing a major role in PDSTP anti-adhesion activity.

Instead, the hypothesized dependency of this activity on PDSTP interaction with host heparan sulfate (HS) appears unlikely based on complementary genetic and enzymatic approaches. Immunofluorescence confirmed abundant HS expression outlining A549 plasma membranes. Flow cytometry highlighted a significantly decreased HS

expression in A549-610 cells, while Heparinase III treatment (50-200 mU/mL) induced dose-dependent HS depletion, partial at 50 mU/mL, near-complete (>90%) at 100-200 mU/mL. Notably, neither intervention substantially altered PAO1 adhesion capacity nor PDSTP's anti-adhesion potency, suggesting that bacterial LPS, rather than host HS, may represent PDSTP's primary molecular target.

Despite these findings, limitations include the focus on laboratory strain PAO1, which may not fully represent mucoid or biofilm-forming clinical isolates from CF patients. The *in vitro* A549 model, while physiologically relevant, lacks the complex CF airway microenvironment.

Future directions should involve *in vivo* validation in CFTR mouse models, testing against multidrug-resistant clinical isolates, and development of PDSTP analogs for improved potency/solubility. Structural studies (cryo-EM of PDSTP-LPS complexes) could enable rational drug design.

In conclusion, this thesis suggests PDSTP may function as a promising LPS-targeting antibiotic adjuvant and anti-adhesion compound for *P. aeruginosa* infections, potentially offering a novel strategy to combat antimicrobial resistance through host-pathogen interface disruption rather than direct bactericidal activity. These findings position PDSTP as a candidate for clinical translation.

BIBLIOGRAPHY

Alimbarova L, Egorova A, Riabova O, Monakhova N, Makarov V. A proof-of-concept study for the efficacy of dispirotripiperazine PDSTP in a rabbit model of herpes simplex epithelial keratitis. Antiviral Res. 2022 Jun;202:105327.

Aggarwal M, Patra A, Awasthi I, George A, Gagneja S, Gupta V, Capalash N, Sharma P. Drug repurposing against antibiotic resistant bacterial pathogens. Eur J Med Chem. 2024 Dec 5;279:116833.

Alqasmi M. Therapeutic Interventions for *Pseudomonas* Infections in Cystic Fibrosis Patients: A Review of Phase IV Trials. J Clin Med. 2024 Oct 30;13(21):6530.

Ambreetha S, Zincke D, Balachandar D, Mathee K. Genomic and metabolic versatility of *Pseudomonas aeruginosa* contributes to its inter-kingdom transmission and survival. J Med Microbiol. 2024 Feb;73(2).

Amin R, Jahnke N, Waters V. Antibiotic treatment for *Stenotrophomonas maltophilia* in people with cystic fibrosis. Cochrane Database Syst Rev. 2020 Mar 18;3(3):CD009249.

Aquino RS, Teng YH, Park PW. Glycobiology of syndecan-1 in bacterial infections. Biochem Soc Trans. 2018 Apr 17;46(2):371-377.

Bjarnsholt T, Jensen PØ, Jakobsen TH, Phipps R, Nielsen AK, Rybtke MT, Tolker-Nielsen T, Givskov M, Høiby N, Ciofu O; Scandinavian Cystic Fibrosis Study Consortium. Quorum sensing and virulence of *Pseudomonas aeruginosa* during lung infection of cystic fibrosis patients. PLoS One. 2010 Apr 12;5(4):e10115.

Blanchard AC, Waters VJ. Microbiology of Cystic Fibrosis Airway Disease. Semin Respir Crit Care Med. 2019 Dec;40(6):727-736.

Bonacorsi A, Trespidi G, Scoffone VC, Irudal S, Barbieri G, Riabova O, Monakhova N, Makarov V, Buroni S. Characterization of the dispirotripiperazine derivative PDSTP as antibiotic adjuvant and antivirulence compound against *Pseudomonas aeruginosa*. Front Microbiol. 2024 Feb 16;15:1357708.

Borisova D, Paunova-Krasteva T, Strateva T, Stoitsova S. Biofilm Formation of *Pseudomonas aeruginosa* in Cystic Fibrosis: Mechanisms of Persistence, Adaptation, and Pathogenesis. Microorganisms. 2025 Jun 30;13(7):1527.

Bouteiller M, Dupont C, Bourigault Y, Latour X, Barbey C, Konto-Ghiorghi Y, Merieau A. *Pseudomonas* Flagella: Generalities and Specificities. Int J Mol Sci. 2021 Mar 24;22(7):3337.

Brooke JS. *Stenotrophomonas maltophilia*: an emerging global opportunistic pathogen. Clin Microbiol Rev. 2012 Jan;25(1):2-41.

Bucior I, Mostov K, Engel JN. *Pseudomonas aeruginosa*-mediated damage requires distinct receptors at the apical and basolateral surfaces of the polarized epithelium. Infect Immun. 2010 Mar;78(3):939-53.

Bucior I, Pielage JF, Engel JN. *Pseudomonas aeruginosa* Pili and Flagella Mediate Distinct Binding and Signaling Events at the Apical and Basolateral Surface of Airway Epithelium. PLoS Pathog. 2012;8(4):e1002616.

Bugli F, Martini C, Di Vito M, Cacaci M, Catalucci D, Gori A, Iafisco M, Sanguinetti M, Vitali A. Antimicrobial peptides for tackling cystic fibrosis related bacterial infections: A review. Microbiol Res. 2022 Oct;263:127152.

Canning JS, Laucirica DR, Ling KM, Nicol MP, Stick SM, Kicic A. Phage therapy to treat cystic fibrosis *Burkholderia cepacia* complex lung infections: perspectives and challenges. Front Microbiol. 2024 Oct 18;15:1476041.

Centers for Disease Control and Prevention. "About *Burkholderia cepacia* complex." Centers for Disease Control and Prevention, U.S. Department of Health & Human Services, 2025, website: https://www.cdc.gov/b-cepacia/about/index.html

Centers for Disease Control and Prevention. "Centers for Disease Control and Prevention." Centers for Disease Control and Prevention, U.S. Department of Health & Human Services, 2022, website: https://www.cdc.gov

Centers for Disease Control and Prevention. "Multidrug-Resistant *Pseudomonas aeruginosa*." Centers for Disease Control and Prevention, U.S. Department of Health & Human Services, 2019, website: https://www.cdc.gov/antimicrobial-resistance/media/pdfs/pseudomonas-aeruginosa-508.pdf

Cervoni M, Sposato D, Lo Sciuto A, Imperi F. Regulatory Landscape of the *Pseudomonas aeruginosa* Phosphoethanolamine Transferase Gene *eptA* in the Context of Colistin Resistance. Antibiotics (Basel). 2023 Jan 18;12(2):200.

CFTR2. "CFTR2 Variant Database." 2025, website: www.cftr2.org

Chen C, Mangoni ML, Di YP. In vivo therapeutic efficacy of frog skin-derived peptides against *Pseudomonas aeruginosa*-induced pulmonary infection. Sci Rep. 2017 Aug 17;7(1):8548.

Cheung GYC, Bae JS, Otto M. Pathogenicity and virulence of *Staphylococcus aureus*. Virulence. 2021 Dec;12(1):547-569.

Cools P, Ho E, Vranckx K, Schelstraete P, Wurth B, Franckx H, Ieven G, Van Simaey L, Van Daele S, Verhulst S, De Baets F, Vaneechoutte M. Epidemic *Achromobacter xylosoxidans* strain among Belgian cystic fibrosis patients and review of literature. BMC Microbiol. 2016 Jun 24;16(1):122.

Cystic Fibrosis Foundation. Cystic Fibrosis Foundation Patient Registry 2024, Annual Data Report. 2025, Bethesda, Maryland.

De Oliveira DMP, Forde BM, Kidd TJ, Harris PNA, Schembri MA, Beatson SA, Paterson DL, Walker MJ. Antimicrobial Resistance in ESKAPE Pathogens. Clin Microbiol Rev. 2020 May 13;33(3):e00181-19.

Denton M, Kerr KG. Microbiological and clinical aspects of infection associated with *Stenotrophomonas maltophilia*. Clin Microbiol Rev. 1998 Jan;11(1):57-80.

Di Bonaventura G, Lupetti V, Di Giulio A, Muzzi M, Piccirilli A, Cariani L, Pompilio A. Repurposing High-Throughput Screening Identifies Unconventional Drugs with Antibacterial and Antibiofilm Activities against *Pseudomonas aeruginosa* under Experimental Conditions Relevant to Cystic Fibrosis. Microbiol Spectr. 2023 Aug 17;11(4):e0035223.

Dickinson KM, Collaco JM. Cystic Fibrosis. Pediatr Rev. 2021 Feb;42(2):55-67.

Drevinek P, Mahenthiralingam E. *Burkholderia cenocepacia* in cystic fibrosis: epidemiology and molecular mechanisms of virulence. Clin Microbiol Infect. 2010 Jul;16(7):821-30.

Duplessis C, Biswas B, Hanisch B, Perkins M, Henry M, Quinones J, Wolfe D, Estrella L, Hamilton T. Refractory *Pseudomonas* Bacteremia in a 2-Year-Old Sterilized by Bacteriophage Therapy. J Pediatric Infect Dis Soc. 2018 Aug 17;7(3):253-256.

Egorova A, Bogner E, Novoselova E, Zorn KM, Ekins S, Makarov V. Dispirotripiperazine-core compounds, their biological activity with a focus on broad antiviral property, and perspectives in drug design (mini-review). Eur J Med Chem. 2021 Feb 5;211:113014.

Elfadadny A, Ragab RF, AlHarbi M, Badshah F, Ibáñez-Arancibia E, Farag A, Hendawy AO, De Los Ríos-Escalante PR, Aboubakr M, Zakai SA, Nageeb WM. Antimicrobial resistance of *Pseudomonas aeruginosa*: navigating clinical impacts, current resistance trends, and innovations in breaking therapies. Front Microbiol. 2024 Apr 5;15:1374466.

Esposito S, Pisi G, Fainardi V, Principi N. What is the role of *Achromobacter* species in patients with cystic fibrosis? Front Biosci (Landmark Ed). 2021; 26(12):1613–1620.

Floto RA, Olivier KN, Saiman L, Daley CL, Herrmann JL, Nick JA, Noone PG, Bilton D, Corris P, Gibson RL, Hempstead SE, Koetz K, Sabadosa KA, Sermet-Gaudelus I, Smyth AR, van Ingen J, Wallace RJ, Winthrop KL, Marshall BC, Haworth CS; US Cystic Fibrosis Foundation and European Cystic Fibrosis Society. US Cystic Fibrosis Foundation and European Cystic Fibrosis Society consensus recommendations for the management of non-tuberculous mycobacteria in individuals with cystic fibrosis. Thorax. 2016 Jan;71 Suppl 1(Suppl 1):i1-22.

Galgano L, Guidetti GF, Torti M, Canobbio I. The Controversial Role of LPS in Platelet Activation *In Vitro*. Int J Mol Sci. 2022;23(18):10900.

García B, Merayo-Lloves J, Martin C, Alcalde I, Quirós LM, Vazquez F. Surface Proteoglycans as Mediators in Bacterial Pathogens Infections. Front Microbiol. 2016; 7:220.

German Center for Infection Research. "Global spread of the multi-resistant pathogen *Stenotrophomonas maltophilia*." German Center for Infection Research, 2020, website: https://www.dzif.de/en/global-spread-multi-resistant-pathogen-stenotrophomonas-maltophilia

Gheorghita AA, Wozniak DJ, Parsek MR, Howell PL. *Pseudomonas aeruginosa* biofilm exopolysaccharides: assembly, function, and degradation. FEMS Microbiol Rev. 2023 Nov 1;47(6):fuad060.

Glajzner P, Bernat A, Jasińska-Stroschein M. Improving the treatment of bacterial infections caused by multidrug-resistant bacteria through drug repositioning. Front Pharmacol. 2024 Jun 7;15:1397602.

Goetz DM, Savant AP. Review of CFTR modulators 2020. Pediatr Pulmonol. 2021 Dec;56(12):3595-3606.

Grace A, Sahu R, Owen DR, Dennis VA. *Pseudomonas aeruginosa* reference strains PAO1 and PA14: A genomic, phenotypic, and therapeutic review. Front Microbiol. 2022 Oct 13;13:1023523.

Gramegna A, Misuraca S, Lombardi A, Premuda C, Barone I, Ori M, Amati F, Retucci M, Nazzari E, Alicandro G, Ferrarese M, Codecasa L, Bandera A, Aliberti S, Daccò V, Blasi F. Treatable traits and challenges in the clinical management of non-tuberculous mycobacteria lung disease in people with cystic fibrosis. Respir Res. 2023 Dec 16;24(1):316.

Gutiérrez Santana JC, Coria Jiménez VR. *Burkholderia cepacia* complex in cystic fibrosis: critical gaps in diagnosis and therapy. Ann Med. 2024 Dec;56(1):2307503.

Hale M, Takehara KK, Thouvenel CD, Moustafa DA, Repele A, Fontana MF, Netland J, McNamara S, Gibson RL, Goldberg JB, Rawlings DJ, Pepper M. Monoclonal antibodies derived from B cells in subjects with cystic fibrosis reduce *Pseudomonas aeruginosa* burden in mice. Elife. 2025 Apr 24;13:RP98851.

Hanssens LS, Duchateau J, Casimir GJ. CFTR Protein: Not Just a Chloride Channel? Cells. 2021 Oct 22;10(11):2844.

Hill UG, Floto RA, Haworth CS. Non-tuberculous mycobacteria in cystic fibrosis. J R Soc Med. 2012 Jun;105 Suppl 2(Suppl 2):S14-8.

Horna G, Ruiz J. Type 3 secretion system of *Pseudomonas aeruginosa*. Microbiol Res. 2021 May;246:126719.

Horspool AM, Sen-Kilic E, Malkowski AC, Breslow SL, Mateu-Borras M, Hudson MS, Nunley MA, Elliott S, Ray K, Snyder GA, Miller SJ, Kang J, Blackwood CB, Weaver KL, Witt WT, Huckaby AB, Pyles GM, Clark T, Al Qatarneh S, Lewis GK, Damron FH, Barbier M. Development of an anti-*Pseudomonas aeruginosa* therapeutic monoclonal antibody WVDC-5244. Front Cell Infect Microbiol. 2023 Apr 14;13:1117844.

Huszczynski SM, Lam JS, Khursigara CM. The Role of *Pseudomonas aeruginosa* Lipopolysaccharide in Bacterial Pathogenesis and Physiology. Pathogens. 2019 Dec 19;9(1):6.

Jacobsen T, Bardiaux B, Francetic O, Izadi-Pruneyre N, Nilges M. Structure and function of minor pilins of type IV pili. Med Microbiol Immunol. 2020 Jun;209(3):301-308.

Jean-Pierre V, Boudet A, Sorlin P, Menetrey Q, Chiron R, Lavigne JP, Marchandin H. Biofilm Formation by *Staphylococcus aureus* in the Specific Context of Cystic Fibrosis. Int J Mol Sci. 2022 Dec 29;24(1):597.

Jennes S, Merabishvili M, Soentjens P, Pang KW, Rose T, Keersebilck E, Soete O, François PM, Teodorescu S, Verween G, Verbeken G, De Vos D, Pirnay JP. Use of bacteriophages in the treatment of colistin-only-sensitive *Pseudomonas aeruginosa* septicaemia in a patient with acute kidney injury-a case report. Crit Care. 2017 Jun 4;21(1):129.

Jia S, Taylor-Cousar JL. Cystic Fibrosis Modulator Therapies. Annu Rev Med. 2023 Jan 27;74:413-426.

Jin Y, Zhou J, Zhou J, Hu M, Zhang Q, Kong N, Ren H, Liang L, Yue J. Genome-based classification of *Burkholderia cepacia* complex provides new insight into its taxonomic status. Biol Direct. 2020 Mar 4;15(1):6.

Jurado-Martín I, Sainz-Mejías M, McClean S. *Pseudomonas aeruginosa*: An Audacious Pathogen with an Adaptable Arsenal of Virulence Factors. Int J Mol Sci. 2021 Mar 18;22(6):3128.

King JD, Kocíncová D, Westman EL, Lam JS. Review: Lipopolysaccharide biosynthesis in *Pseudomonas aeruginosa*. Innate Immun. 2009 Oct;15(5):261-312.

Konings AF, Martin LW, Sharples KJ, Roddam LF, Latham R, Reid DW, Lamont IL. *Pseudomonas aeruginosa* uses multiple pathways to acquire iron during chronic infection in cystic fibrosis lungs. Infect Immun. 2013 Aug;81(8):2697-704.

Kramer-Golinkoff E, Camacho A, Kramer L, Taylor-Cousar JL. A survey: Understanding the health and perspectives of people with CF not benefiting from CFTR modulators. Pediatr Pulmonol. 2022 May;57(5):1253-1261.

Lam JS, Taylor VL, Islam ST, Hao Y, Kocíncová D. Genetic and Functional Diversity of *Pseudomonas aeruginosa* Lipopolysaccharide. Front Microbiol. 2011 Jun 1;2:118.

Langton Hewer SC, Smyth AR. Antibiotic strategies for eradicating *Pseudomonas aeruginosa* in people with cystic fibrosis. Cochrane Database Syst Rev. 2017 Apr 25;4(4):CD004197.

Lee J, Zhang L. The hierarchy quorum sensing network in *Pseudomonas aeruginosa*. Protein Cell. 2015 Jan;6(1):26-41.

Lee JA, Cho A, Huang EN, Xu Y, Quach H, Hu J, Wong AP. Gene therapy for cystic fibrosis: new tools for precision medicine. J Transl Med. 2021 Oct 30;19(1):452.

Li D, Schneider-Futschik EK. Current and Emerging Inhaled Antibiotics for Chronic Pulmonary *Pseudomonas aeruginosa* and *Staphylococcus aureus* Infections in Cystic Fibrosis. Antibiotics (Basel). 2023 Feb 28;12(3):484.

Li H, Luo YF, Williams BJ, Blackwell TS, Xie CM. Structure and function of OprD protein in *Pseudomonas aeruginosa*: from antibiotic resistance to novel therapies. Int J Med Microbiol. 2012 Mar;302(2):63-8.

Liao C, Huang X, Wang Q, Yao D, Lu W. Virulence Factors of *Pseudomonas aeruginosa* and Antivirulence Strategies to Combat Its Drug Resistance. Front Cell Infect Microbiol. 2022 Jul 6;12:926758.

Lister PD, Wolter DJ, Hanson ND. Antibacterial-resistant *Pseudomonas aeruginosa*: clinical impact and complex regulation of chromosomally encoded resistance mechanisms. Clin Microbiol Rev. 2009 Oct;22(4):582-610.

Lopes-Pacheco M. CFTR Modulators: The Changing Face of Cystic Fibrosis in the Era of Precision Medicine. Front Pharmacol. 2020 Feb 21;10:1662.

Lord R, Jones AM, Horsley A. Antibiotic treatment for *Burkholderia cepacia* complex in people with cystic fibrosis experiencing a pulmonary exacerbation. Cochrane Database Syst Rev. 2020 Apr 2;4(4):CD009529.

Lorusso AB, Carrara JA, Barroso CDN, Tuon FF, Faoro H. Role of Efflux Pumps on Antimicrobial Resistance in *Pseudomonas aeruginosa*. Int J Mol Sci. 2022 Dec 13;23(24):15779.

Lund-Palau H, Turnbull AR, Bush A, Bardin E, Cameron L, Soren O, Wierre-Gore N, Alton EW, Bundy JG, Connett G, Faust SN, Filloux A, Freemont P, Jones A, Khoo V, Morales S, Murphy R, Pabary R, Simbo A, Schelenz S, Takats Z, Webb J, Williams HD, Davies JC. *Pseudomonas aeruginosa* infection in cystic fibrosis: pathophysiological mechanisms and therapeutic approaches. Expert Rev Respir Med. 2016 Jun;10(6):685-97.

Menetrey Q, Sorlin P, Jumas-Bilak E, Chiron R, Dupont C, Marchandin H. *Achromobacter xylosoxidans* and *Stenotrophomonas maltophilia*: Emerging Pathogens Well-Armed for Life in the Cystic Fibrosis Patients' Lung. Genes (Basel). 2021 Apr 21;12(5):610.

Minandri F, Imperi F, Frangipani E, Bonchi C, Visaggio D, Facchini M, Pasquali P, Bragonzi A, Visca P. Role of Iron Uptake Systems in *Pseudomonas aeruginosa* Virulence and Airway Infection. Infect Immun. 2016 Jul 21;84(8):2324-2335.

Mitri C, Xu Z, Bardin P, Corvol H, Touqui L, Tabary O. Novel Anti-Inflammatory Approaches for Cystic Fibrosis Lung Disease: Identification of Molecular Targets and Design of Innovative Therapies. Front Pharmacol. 2020 Jul 23;11:1096.

Moskowitz SM, Ernst RK, Miller SI. PmrAB, a two-component regulatory system of *Pseudomonas aeruginosa* that modulates resistance to cationic antimicrobial peptides and addition of aminoarabinose to lipid A. J Bacteriol. 2004 Jan;186(2):575-9.

Muggeo A, Coraux C, Guillard T. Current concepts on *Pseudomonas aeruginosa* interaction with human airway epithelium. PLoS Pathog. 2023 Mar 30;19(3):e1011221.

Mulani MS, Kamble EE, Kumkar SN, Tawre MS, Pardesi KR. Emerging Strategies to Combat ESKAPE Pathogens in the Era of Antimicrobial Resistance: A Review. Front Microbiol. 2019 Apr 1;10:539.

Murphy RA, Coates M, Thrane S, Sabnis A, Harrison J, Schelenz S, Edwards AM, Vorup-Jensen T, Davies JC. Synergistic Activity of Repurposed Peptide Drug Glatiramer Acetate with Tobramycin against Cystic Fibrosis *Pseudomonas aeruginosa*. Microbiol Spectr. 2022 Aug 31;10(4):e0081322.

Örlős Z, Lőrinczi LK, Antus B, Barta I, Miklós Z, Horváth I. Epidemiology, microbiology and clinical impacts of non-tuberculous mycobacteria in adult patients with cystic fibrosis. Heliyon. 2024 Dec 17;11(1):e41324.

Pang Z, Raudonis R, Glick BR, Lin TJ, Cheng Z. Antibiotic resistance in *Pseudomonas aeruginosa*: mechanisms and alternative therapeutic strategies. Biotechnol Adv. 2019 Jan-Feb;37(1):177-192.

Petrocheilou A, Moudaki A, Kaditis AG. Inflammation and Infection in Cystic Fibrosis: Update for the Clinician. Children (Basel). 2022 Dec 2;9(12):1898.

Polgreen PM, Comellas AP. Clinical Phenotypes of Cystic Fibrosis Carriers. Annu Rev Med. 2022 Jan 27;73:563-574.

Qian Y, Zhou D, Li M, Zhao Y, Liu H, Yang L, Ying Z, Huang G. Application of CRISPR-Cas system in the diagnosis and therapy of ESKAPE infections. Front Cell Infect Microbiol. 2023 Aug 17;13:1223696.

Radlović N. Cystic fibrosis. Srp Arh Celok Lek. 2012 Mar-Apr;140(3-4):244-9.

Ratjen F, Bell SC, Rowe SM, Goss CH, Quittner AL, Bush A. Cystic fibrosis. Nat Rev Dis Primers. 2015 May 14;1:15010.

Regard L, Martin C, Burnet E, Da Silva J, Burgel PR. CFTR Modulators in People with Cystic Fibrosis: Real-World Evidence in France. Cells. 2022 May 28;11(11):1769.

Riordan JR, Rommens JM, Kerem B, Alon N, Rozmahel R, Grzelczak Z, Zielenski J, Lok S, Plavsic N, Chou JL, Drumm ML, Iannuzzi MC, Collins FS, Tsui L. Identification of the cystic fibrosis gene: cloning and characterization of complementary DNA. Science. 1989 Sep 8;245(4922):1066-73.

Rumpf C, Lange J, Schwartbeck B, Kahl BC. *Staphylococcus aureus* and Cystic Fibrosis-A Close Relationship. What Can We Learn from Sequencing Studies? Pathogens. 2021 Sep 13;10(9):1177.

Sahl C, Baumgarten M, Shannon O, Påhlman LI. Exoproducts of the Most Common *Achromobacter* Species in Cystic Fibrosis Evoke Similar Inflammatory Responses *In Vitro*. Microbiol Spectr. 2023 Aug 17;11(4):e0019523.

Sankari A, Sharma S. Cystic Fibrosis. 2024 Dec 11. In: StatPearls [Internet]. Treasure Island (FL): StatPearls Publishing; 2025 Jan–.

Sanna G, Riabova O, Kazakova E, Lepioshkin A, Monakhova N, Marongiu A, Franci G, Manzin A, Makarov V. Efficacy of dispirotripiperazine PDSTP in a golden Syrian hamster model of SARS-CoV-2 infection. Front Microbiol. 2025 Mar 10;16:1546946.

Sarrazin S, Lamanna WC, Esko JD. Heparan sulfate proteoglycans. Cold Spring Harb Perspect Biol. 2011 Jul 1;3(7):a004952.

Sharma SK, Upadhyay V. Epidemiology, diagnosis & treatment of non-tuberculous mycobacterial diseases. Indian J Med Res. 2020 Sep;152(3):185-226.

Siddam AD, Zaslow SJ, Wang Y, Phillips KS, Silverman MD, Regan PM, Amarasinghe JJ. Characterization of Biofilm Formation by *Mycobacterium chimaera* on Medical Device Materials. Front Microbiol. 2021 Jan 11;11:586657.

Sousa SA, Seixas AMM, Marques JMM, Leitão JH. Immunization and Immunotherapy Approaches against *Pseudomonas aeruginosa* and *Burkholderia cepacia* Complex Infections. Vaccines (Basel). 2021 Jun 18;9(6):670.

Terlizzi V, Tomaselli M, Giacomini G, Dalpiaz I, Chiappini E. *Stenotrophomonas maltophilia* in people with Cystic Fibrosis: a systematic review of prevalence, risk factors and management. Eur J Clin Microbiol Infect Dis. 2023 Nov;42(11):1285-1296.

Thi MTT, Wibowo D, Rehm BHA. *Pseudomonas aeruginosa* Biofilms. Int J Mol Sci. 2020 Nov 17;21(22):8671.

Thornton CS, Parkins MD. Microbial Epidemiology of the Cystic Fibrosis Airways: Past, Present, and Future. Semin Respir Crit Care Med. 2023 Apr;44(2):269-286.

Tomás M, Doumith M, Warner M, Turton JF, Beceiro A, Bou G, Livermore DM, Woodford N. Efflux pumps, OprD porin, AmpC beta-lactamase, and multiresistance in *Pseudomonas aeruginosa* isolates from cystic fibrosis patients. Antimicrob Agents Chemother. 2010 May;54(5):2219-24.

Torrens G, Hernández SB, Ayala JA, Moya B, Juan C, Cava F, Oliver A. Regulation of AmpC-Driven β-Lactam Resistance in *Pseudomonas aeruginosa*: Different Pathways, Different Signaling. mSystems. 2019 Dec 3;4(6):e00524-19.

Tuon FF, Dantas LR, Suss PH, Tasca Ribeiro VS. Pathogenesis of the *Pseudomonas aeruginosa* Biofilm: A Review. Pathogens. 2022 Feb 27;11(3):300.

Vaziri F, Peerayeh SN, Nejad QB, Farhadian A. The prevalence of aminoglycoside-modifying enzyme genes (aac (6')-I, aac (6')-II, ant (2")-I, aph (3')-VI) in *Pseudomonas aeruginosa*. Clinics (Sao Paulo). 2011;66(9):1519-22.

Zhang Y, Zhang T, Xiao X, Wang Y, Kawalek A, Ou J, Ren A, Sun W, de Bakker V, Liu Y, Li Y, Yang L, Ye L, Jia N, Veening JW, Liu X. CRISPRi screen identifies FprB as a synergistic target for gallium therapy in *Pseudomonas aeruginosa*. Nat Commun. 2025 Jul 1;16(1):5870.

Zolin A, Adamoli A, Bakkeheim E. ECFSPR Annual Report 2023. 2025.